Research Highlight

[FY2021]

Japan International Research Center for Agricultural Sciences

Meeting global challenges through research and technology development

JIRCAS
国際農研

Multiple drainage can cancel out the enhancement of methane emission by biogas effluent application in a rice paddy

Household biogas production from livestock manure and its domestic use in cooking and heating is popular in Vietnam. However, the discharge of untreated biogas effluent (also known as methane fermentation digestate) containing plant nutrients, including nitrogen, into rivers causes local environmental problems such as water pollution. To address this issue, the biogas effluent was used as organic fertilizer for rice, the locally dominant crop, and was found to be effective (2019 Research Highlights article entitled "Variable-timing, fixed-rate application of cattle biogas effluent as fertilizer for rice using a leaf color chart"). However, because biogas effluent also contains labile organic carbon, which is a substrate for microbial production of methane (CH_4), a potent greenhouse gas (GHG), its application to a paddy field may enhance CH_4 emission from the flooded soil. Here we hypothesized that combining multiple drainage with biogas effluent application can cancel out the CH_4 enhancement, and tested this by observing a farmer's paddy field with triple rice cropping in the Mekong Delta, Vietnam.

Chemical properties, including organic matter content, of the biogas effluent produced from cattle manure varied among rice seasons, and the application of cattle biogas effluent increased CH_4 emission by 19% on average as compared to synthetic fertilizer application (Fig. 1). We tested two multiple drainage practices: alternate wetting and drying (AWD), which is a water-depth-dependent irrigation method; and midseason drainage followed by intermittent irrigation (MiDi), which is a day-number-dependent irrigation method. Although the lowland location made it difficult to naturally drain flooded surface water, both AWD and MiDi reduced CH_4 emission in proportion to the increase in the number of drained days between crop establishment and final drainage in each rice season (Fig. 2). As a result, the proposed combination practices reduced CH_4 emission by 11–13% and nitrous oxide (N_2O), another potent GHG, emission by 35–54% without loss of grain and straw yields as compared to the conventional practice with synthetic fertilizer application and continuous flooding (Fig. 3). The Global Warming Potential (GWP), carbon dioxide (CO_2)-equivalent of combined CH_4 and N_2O emissions, and grain-yield-scaled GWP were also reduced by the proposed combination practices.

The results indicate that the proposed combination practice (i.e., multiple drainage with biogas effluent application) can be applied to the rice-producing areas using livestock biogas effluent as organic fertilizer. It is likely that multiple drainage can further reduce CH_4 emission in case of a field location under better drainage conditions.

(K. Minamikawa, K. Uno,
K.C. Huynh [Can Tho University, Vietnam (CTU)], N.S. Tran [CTU], C.H. Nguyen [CTU])

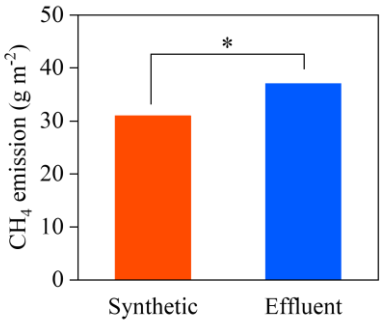

Fig. 1. CH_4 emissions from synthetic fertilizer application and biogas effluent application

Statistically significant difference at $p < 0.05$ by ANOVA.

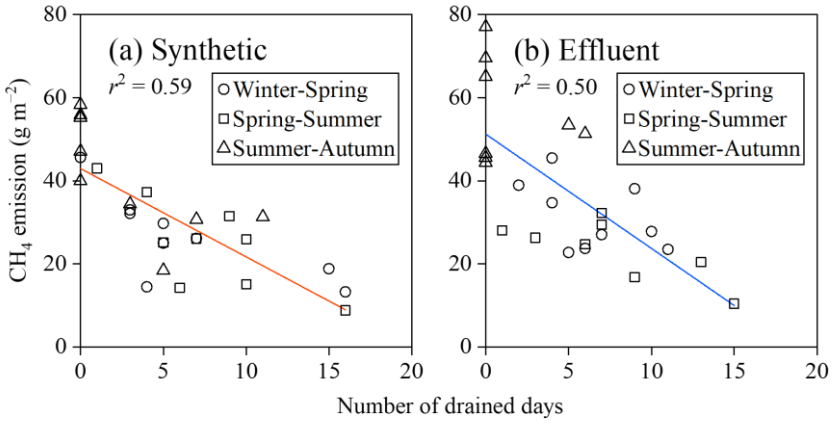

Fig. 2. Relationships between CH_4 emission and the number of drained days between crop establishment and final drainage in each rice season for (a) synthetic fertilizer application and (b) biogas effluent application

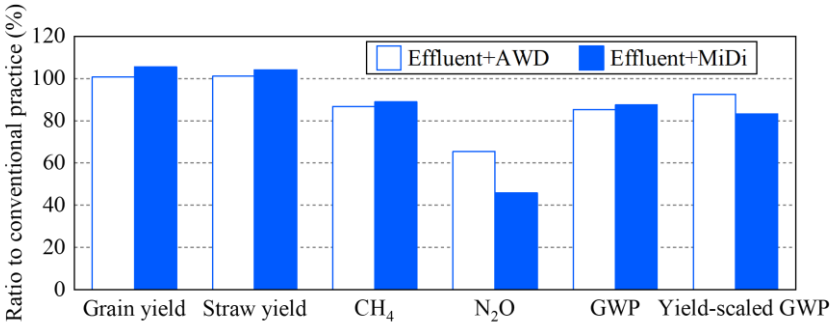

Fig. 3. Comparisons between the proposed combination practices, biogas effluent application with AWD or MiDi, and the conventional practice with synthetic fertilizer application and continuous flooding

Reference: Minamikawa K et al. (2021) *Agriculture, Ecosystems and Environment* 319: 107568

Figures reprinted/modified with permission.

Water requirement of ratoon rice is larger in the early growth stage and smaller in the late growth stage compared to transplanted rice

Actual crop evapotranspiration (ET) and crop coefficients (Kc values) are necessary for ratoon rice crop irrigation planning, but these data have been hardly reported. Kc is usually determined experimentally, using ET values measured by lysimeters and eddy covariance. However, especially in developing countries, determining Kc remains difficult because ET observation systems are expensive. The focus of this study, therefore, was to evaluate the ET and Kc of ratoon cropping in a tropical region of Myanmar using a simplified method.

Our method combined the manual observation of water depth in concrete paddy tanks (1.62 m L × 0.84 m W × 0.4 m D on the inside of tank) and the ET model estimation using Bayesian parameter inference with meteorological data. The difference in daily pond water depth (mm day^{-1}) above the soil surface in a tank with and without planting rice are defined as daily ET and evaporation (E), respectively. When it rains, the daily pond water depth cannot be measured because the water balance in the tank is unknown. The missing ET and E values could be interpolated with modeled values by statistical modeling to determine the Kc values (Fig. 1).

The ratios of ET and E of ratoon crop to main crop (59% and 55% for the rainy season and 74% and 82% for the cool and dry season) were almost equivalent for both seasons (Fig. 2). Thus, the difference in the ET between main crop and ratoon was mainly attributed to the difference in climate conditions in each cropping period. The R^2 of the transplanted rice was higher than that of the ratoon in number of tillers with the accumulated temperature. The transplanted rice reached the maximum tillering period at about 1,500°C accumulated temperature. On the other hand, the ratoon had vigorous tillering with large variations in the initial growth stage (Fig. 3). Consequently, the Kc regression curves for transplanted rice and ratoon crops were considerably different because of the difference in tillering traits (Fig. 4). The results suggest that irrigation scheduling of ratoon rice cropping should take into account higher crop water requirements in the initial growth stage and less water consumption in the late growth stage than transplanted rice cropping.

(S. Shiraki, Thin Mar Cho [Department of Agricultural Research (DAR), Myanmar])

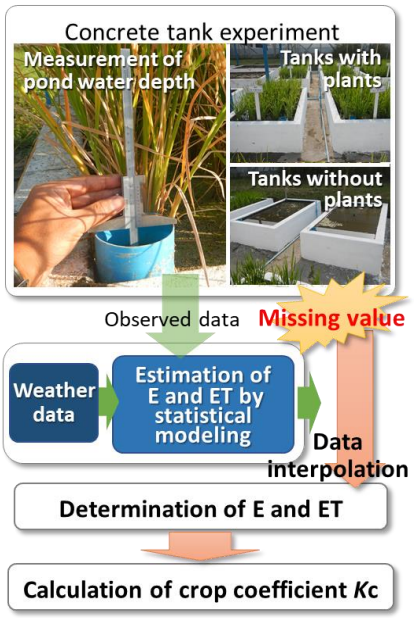

Fig. 1. Calculation procedure for crop coefficient Kc

Weather data indicate the net radiation, air temperature, humidity, and wind speed.

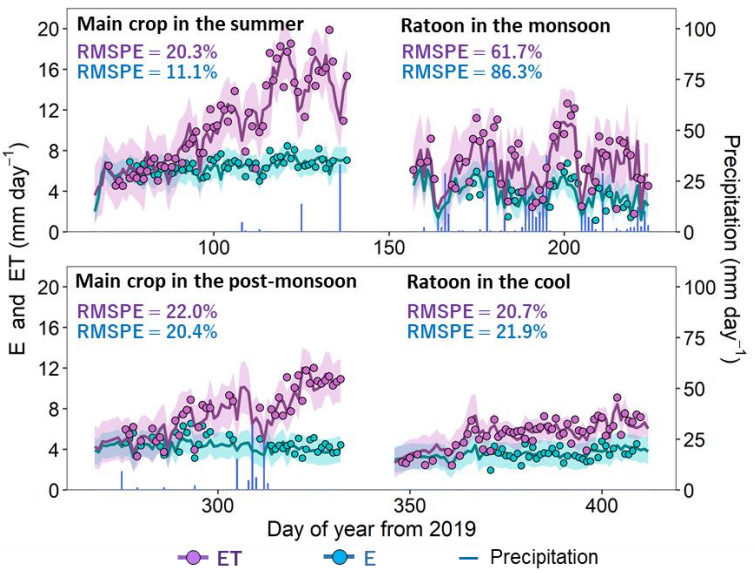

Fig. 2. Observed and estimated E and ET in ratoon double rice cropping in different seasons

The periods of the first and second double cropping are February 2019 to August 2019 and September 2019 to April 2020, respectively. The model estimates are described with lines and bands corresponding to the means and 95% credible intervals. RMSPE, root mean squared percentage error.

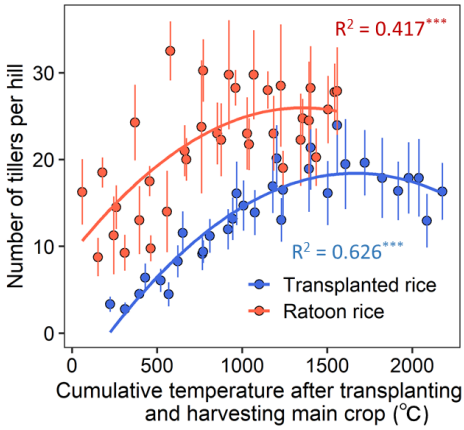

Fig. 3. Comparison of the cumulative temperature and number of tillers per hill described with non-linear bands and dots with bars

The error bars, the standard errors (n = 4∼8); R^2, determination coefficient; ***, 0.001% significance level.

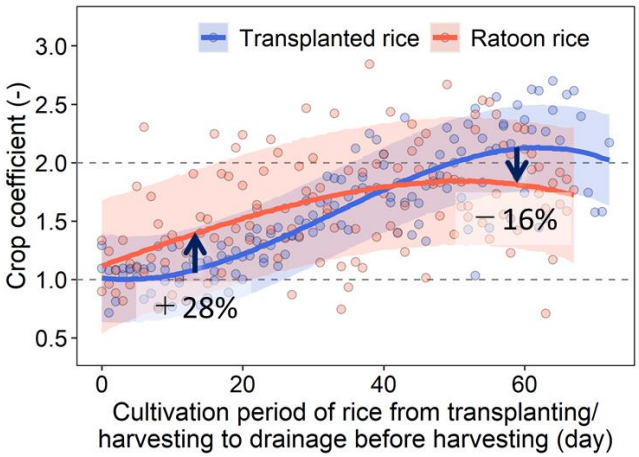

Fig. 4. Kc regression curves for transplanted and ratoon rice described with lines and bands corresponding to the means and 95% credible intervals (transplanted rice: n = 138, ratoon: n = 135)

Values with percent in the figure is the increase-decrease rate in the Kc of ratoon rice with transplanted rice.

Reference: Shiraki et al. (2021) *Agronomy* 11(8):1573. https://doi.org/10.3390/agronomy11081573

Effect of conventionally decomposed oil palm trunks on the soil environment

Oil palm fruit is harvested 3 years after planting until the harvest yield declines at around 25 years, and oil palms need to be replanted at an interval of 25–30 years to maintain oil productivity. Oil palm trunks (OPTs) are logged for replantation and the fiber residues are disposed of into the palm plantation area. The fiber residues are expected to increase soil fertility through recycling of carbon and minerals via fiber decomposition. However, the unregulated disposal of OPT can have detrimental effects on soil functioning and plant growth. To understand the effect of OPT fiber on the soil environment, this study compared corn, tomato, and bean plant growth and nutrient availability in soil mixed with OPT fiber and other comparable soil amendments using cellulose powder.

(A) soil+OPT fiber (1:20), (B) soil+cellulose powder (1:20), and (C) unamended soil as a negative control plot were prepared and tested. The effect of amendment with OPT fiber on plant growth was compared in a pot experiment. In the period after 25 days after sowing, the low chlorophyll contents were consistent with the symptoms of nutritional disorders such as yellowish leaves and stunting of height. Furthermore, OPT fiber treatments caused a reduction in heights and SPAD values (chlorophyll content), with a maximum reduction of 54.9% of the height and 58.8% of SPAD compared with plants grown in the control soil. The dry weight of biomass was reduced by 53.3% for the OPT fiber treatment when compared with the control (Fig. 1). The plants grown with OPT fiber were deficient in total nitrogen and magnesium when compared with those without fiber amendment, which suggested that nitrogen and minerals in the soil might be taken up by the changing microflora because of the OPT fibers' presence (Table 1). To confirm the differences in the soil microflora, metagenomics analysis was performed on untreated soil and soil from each lignocellulose treatment. The microflora of soils mixed with OPT fiber and cellulose revealed substantial increases in bacteria such as families *Cytophagaceae* and *Oscillospiraceae*, and two major fungal genera, *Trichoderma* and *Trichocladium*, that are involved in lignocellulose degradation. OPT fiber resulted in a drastic increase in the ratios and amounts of *Trichocladium* in the soil when compared with those of cellulose treatments (Fig. 2).

These results indicate that unregulated disposal of OPT fiber into plantation areas could result in nutrient loss from soil by increasing the abundance of microorganisms involved in lignocellulose decomposition. To protect palm plantation productivity, co-composting of these biomass products or re-using OPT for other products is necessary.

A. Uke, A. Kosugi,
J-A. Chuah [Universiti Sains Malaysia, USM] K. Sudesh [USM],
N.Z.H.A.Z. Abidin [Malaysian Palm Oil Board, MPOB], Z. Hashim [MPOB])

Table 1. Plant analysis results of plants grown in unamended soil and soil supplemented with oil plant trunk (OPT) fiber

Elements	Corn		Tomato		Beans	
	Unamended	OPT fiber	Unamended	OPT fiber	Unamended	OPT fiber
Potassium (P)	0.09%	0.07%	0.11%	0.18%	0.08%	0.09%
Magnesium (Mg)	0.25%	0.17%	1.18%	0.70%	0.60%	0.53%
Phosphorus (K)	3.16%	2.91%	3.49%	3.75%	1.32%	1.42%
Total nitrogen (N)	2.09%	0.73%	3.36%	1.56%	1.58%	0.68%
Inorganic nitrogen	0.24%	0.01%	0.22%	0.01%	0.02%	0.01%

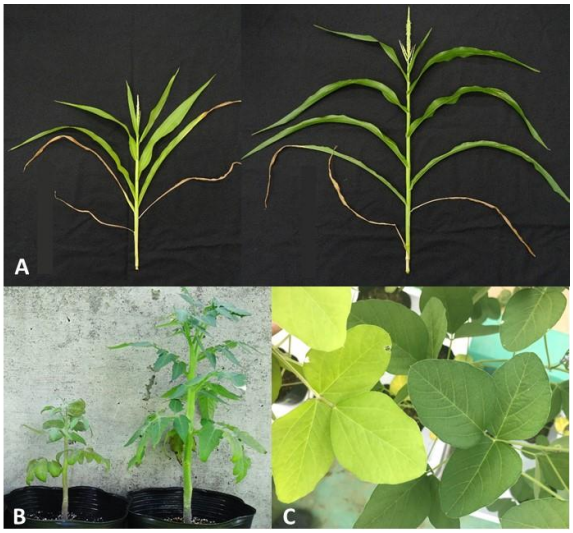

Fig. 1. Growth trend of plants

A: corn, B: tomato, C: beans. Left: soil mixed with OPT fiber (OPT fiber), right: soil not mixed with OPT fiber (unamended soil).

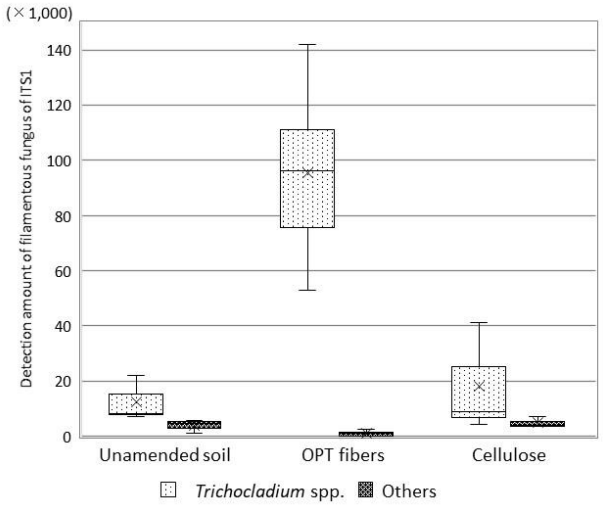

Fig. 2. Microbial relative abundance of sequences from unamended soil, OPT fibers, and cellulose

The ITS region sequence amount of *Trichocladium* spp. and other filamentous fungi generated by metagenome is shown. As a control, the soil mixed with cellulose (manufactured by Sigma-Aldrich) is shown.

Reference: Uke A et al. (2021) *Journal of Environmental Management*, 295:113050

BNI-enabled wheat is nitrogen-efficient and maintains productivity

The amount of nitrogen fertilizer used in modern agriculture is enormous, amounting to about 120 million tons worldwide. However, most of it (about 70%) is not absorbed by crops and is leached out from farmland, making farmland a source of pollution to the aquatic environment and emission of nitrous oxide (N_2O), a global warming gas with a greenhouse effect up to 298 times greater than that of carbon dioxide. The release of excess nitrogen into the environment is related to nitrification in the soil. Nitrification is a microbial oxidation reaction from ammonia-form nitrogen (NH_4^+-N) to nitrate-form nitrogen (NO_3^--N), which is an important pathway in the nitrogen cycle of the earth. $NH4^+$ is retained in the soil and does not migrate much, while NO_3^- is weakly bound to the soil and is highly mobile, so it easily leaches out of the farmland. Nitrification in agricultural soils is highly active due to a large amount of industrially fixed nitrogen fertilizer applied, so the conversion to NO_3^-, which cannot be retained by the soil, and its leaching into the hydrosphere proceed rapidly, and N_2O is released into the atmosphere during the process (Fig. 1 left).

Therefore, if the nitrification rate of agricultural soil can be suppressed, it could be an effective means of solving the problem. Biological Nitrification Inhibition (BNI) is the process by which crops themselves secrete substances that inhibit nitrification. BNI technology that utilizes BNI can both maintain and increase crop yields with less nitrogen fertilizer input and reduce environmental impact. By inhibiting nitrification, crops have more opportunities to absorb nitrogen, which allows reducing NO_3^- leaching and N_2O release. The introduction or enhancement of BNI capacity through breeding can be expected to both reduce agricultural greenhouse gas emissions and nitrogen fertilizer application.

We have been investigating the BNI potential of wheat, a major cereal covering the largest area among food crops, and developed BNI-enabled wheat by introducing superior BNI capacity from *Leymus racemosus* into high-yielding wheat varieties through chromosome engineering tools. Substitution of *Leymus racemosus* chromosome N short-arm with wheat chromosome 3B introduced BNI capacity, and the resulting line was further back-crossed with high-yielding varieties. (Fig. 2) The BNI-enabled variety, “BNI-Munal,” showed around 2–5 times higher BNI capacity than the parental variety, “Munal.” This high-yielding background ”BNI-Munal” showed suppression of nitrifying microorganisms in rhizosphere soil, resulting in the lowering of soil nitrification rate and N_2O emission (Fig. 3); therefore, the environmental load by agriculture caused by nitrogen fertilizer can be reduced. “BNI-Munal” also showed efficient use of NH_4^+ in terms of nitrogen assimilation and soil organic nitrogen. “BNI-Munal” showed a significantly higher yield than Munal, and a 60% reduction in nitrogen application (from 250 to 100 kgN/ha) did not show a difference in yield between BNI-enabled and parental variety, hence the grain protein content (and bread-making quality) also did not change (Fig. 3). Further improvement in BNI capacity can be made by reducing the N chromosome short-arm and elucidating the mode of action, which is ongoing.

(G. V. Subbarao, M. Kishii, T. Yoshihashi, S. Tobita [Nihon Univ.], M. Iwanaga and 9 others)

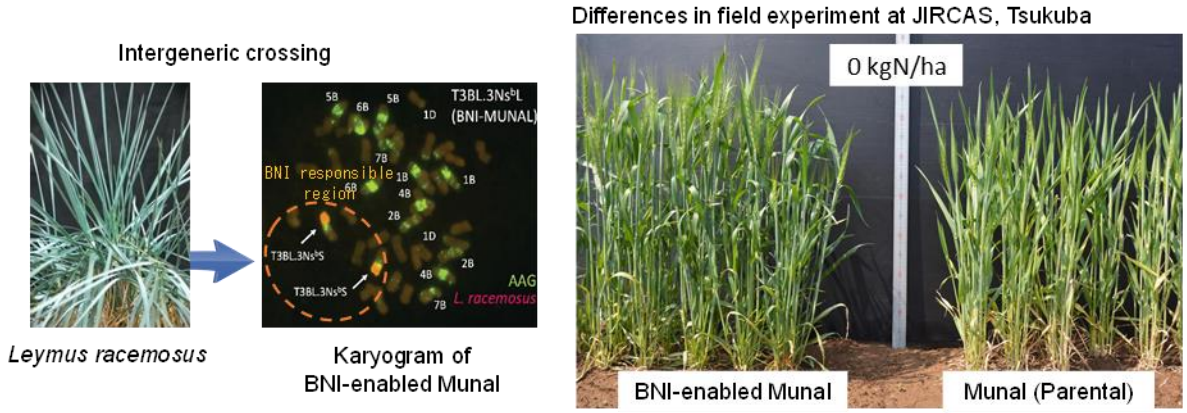

Fig. 1. BNI-enabled wheat with *Leymus racemosus* N chromosome (ex. BNI-Munal)

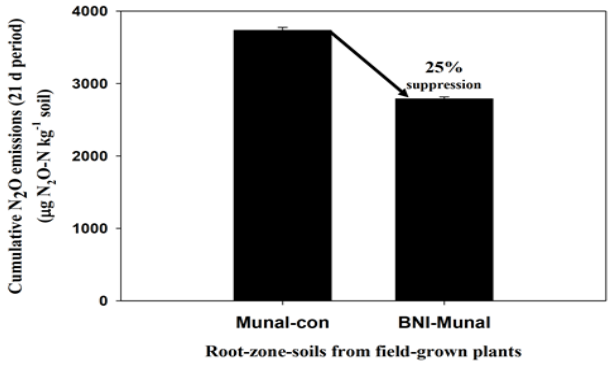

Fig. 2. N_2O emission from BNI-enabled Munal

N_2O emission was suppressed by 25%.

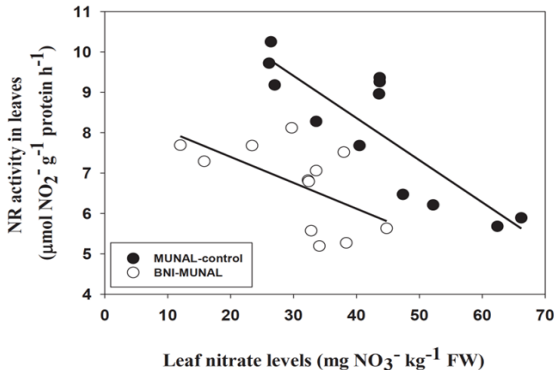

Fig. 3. Changes in nitrogen assimilation

BNI-enabled wheat prefers ammonium.

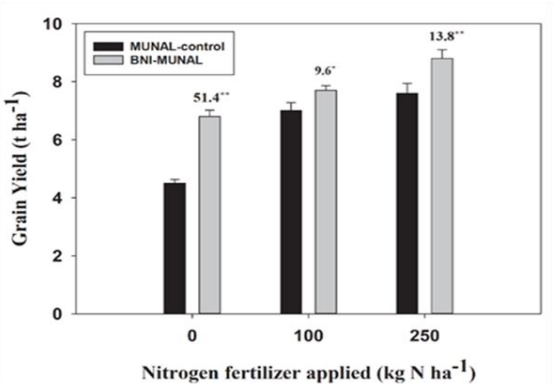

Fig. 4. Grain yield under different nitrogen application levels

No significant difference in yields between Munal-control at 250 kg/ha and BNI-enabled Munal at 100 kg/ha.

Fig. 5. Bread making quality of BNI-enabled wheat

BNI-enabled Munal can be processed into bread as well as Munal-control.

Reference: Subbarao et al. (2021) *PNAS* 118: e2106595118, https://doi.org.10.1073/pnas.2106595118

Discovery of biological nitrification inhibitors in maize roots

Nitrogen (N) fertilizer is an essential component for growing most crop plants. However, almost half of the applied N fertilizer is lost from soil as nitrate (NO_3^-, a water pollutant) and as nitrous oxide (N_2O, a greenhouse gas) by two microbial metabolic processes: nitrification and denitrification, respectively. To control agronomic N losses, biological nitrification inhibition (BNI) is a promising strategy. BNI is an ecological phenomenon by which certain plants release bioactive natural products that can suppress nitrifying soil microbes. Our objective in this research is the identification of hydrophobic BNI compounds released from maize roots.

In the search for BNI compounds from the surface extract of maize roots, a new highly BNI active compound was discovered, together with a highly active compound. In addition, two BNI active compounds were identified from the root extract of maize (Fig. 1). The compound with the strongest BNI activity (the ability to suppress nitrification by nitrifying bacteria) was named “zeanone” because it was the first BNI compound to be discovered in nature. The four compounds, including the newly discovered zeanone, were found to have an activity equivalent to 45% of the total BNI activity of maize roots (Table 1). Based on the obtained results, a BNI mechanism in maize is proposed (Fig. 2).

The results of this research are expected to open the way for the construction of eco-friendly agricultural production systems that utilize the BNI-producing ability (BNI capacity) of maize.

(J. Otaka, T. Yoshihashi, G. V. Subbarao,
H. Ono [National Agriculture and Food Research Organization])

Table 1. Quantity of BNI compounds in maize roots

Compound	Root surface (220 mg)	Root inside DCM extract (395 mg)	Root inside MeOH extract (10 g)	Root (10.615 g)
Zeanone	0.1 mg	0.05 mg	–	0.15 mg (19% of total BNI activity)
HDMBOA	110 mg	132 mg	–	242 mg (20% of total BNI activity)
HMBOA	–	–	3.0 mg	3.0 mg (2% of total BNI activity)
HDMBOA-β-glc	–	–	20 mg	20 mg (4% of total BNI activity)

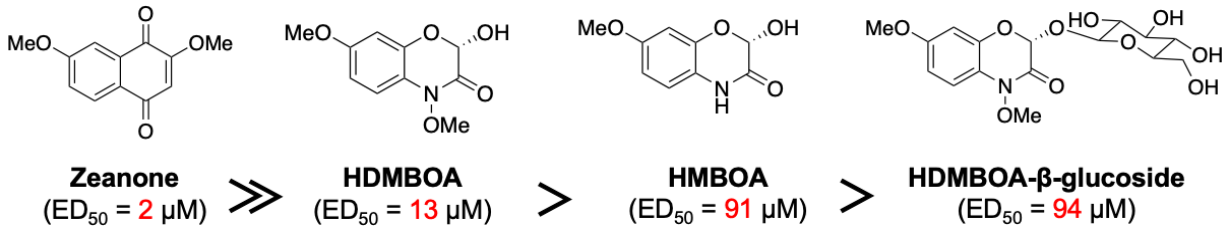

Fig. 1. Structure and BNI activity of BNI compounds

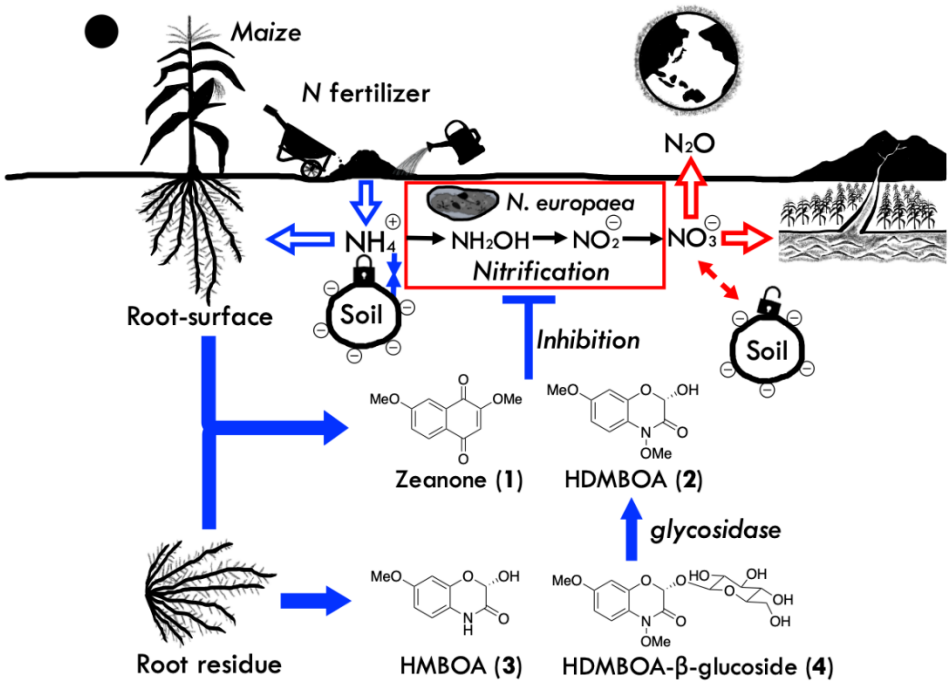

Fig. 2. Proposed BNI mechanism in maize

Reference: Otaka et al. (2021) *Biol Fertil Soils* 58: 251−264, https://doi.org/10.1007/s00374-021-01577-x

Figures and table reprinted/modified with permission.

Reduction in nitrogen fertilizer-induced greenhouse gas emissions by BNI-enabled wheat

Since the beginning of the "Green Revolution," nitrogen (N) fertilizer consumption worldwide has increased ninefold. Soil nitrifier activity and nitrification have been increased by high fertilization rates, resulting in declining agronomic N-use efficiency (NUE) and an increase in environmental problems. The agronomic NUE for cereals is reported to be 30–50%. The remaining N is partially lost to the environment, exacerbating groundwater pollution by nitrate and climate change by nitrous oxide (N_2O) emissions from farmlands.

To increase NUE and to reduce the detrimental effects of reactive N on the environment, JIRCAS has focused on the release of root exudates from plants, a mechanism known as "Biological Nitrification Inhibition (BNI)." In collaboration with the International Center for Maize and Wheat Improvement (CIMMYT), JIRCAS has developed BNI-enabled wheat with a 30% nitrification inhibition rate. Aiming to reach carbon neutrality by 2050, the research team is currently developing BNI-enabled elite wheat varieties with a 40% reduction in nitrification.

Thus far, the potential impacts of deploying BNI-enabled elite wheat in wheat production systems have yet to be evaluated. The present study aims to evaluate the potential changes in fertilizer application rates, life cycle greenhouse gas (LC-GHG) emissions (Fig. 1), and NUE at the farm level. Moreover, it aims to evaluate the potential changes in worldwide nitrogen fertilizer-induced GHG emissions across wheat-harvested areas.

The study showed that BNI-enabled wheat with a 30% reduction in nitrification could reduce LC-GHG emissions by 12.3% and N fertilization by 11.7%, and improve NUE by 12.5% at the farm level by 2030 (Fig. 2, 30%). Furthermore, BNI-enabled wheat with a 40% reduction in nitrification could reduce LC-GHG emissions by 15.9% and N fertilization by 15.0%, and improve NUE by 16.7% by 2050 (Fig. 2, 40%). In addition, N fertilizer-induced GHG emissions could be reduced by 9.5% across wheat-harvested areas worldwide by 2050 if BNI-enabled wheat with a 40% reduction in nitrification is introduced only to areas suitable for BNI wheat (Fig. 3).

JIRCAS, together with CIMMYT, has presented estimates on the development of BNI-enabled wheat, which can reduce fertilizer use and GHG emissions, and will promote the use of BNI-enabled wheat in wheat-producing countries to achieve both high productivity and reduced environmental load from agriculture.

(A. Leon, G.V. Subbarao, N. Matsumoto, M. Kishii,
G. Kruseman [International Maize and Wheat Improvement Center])

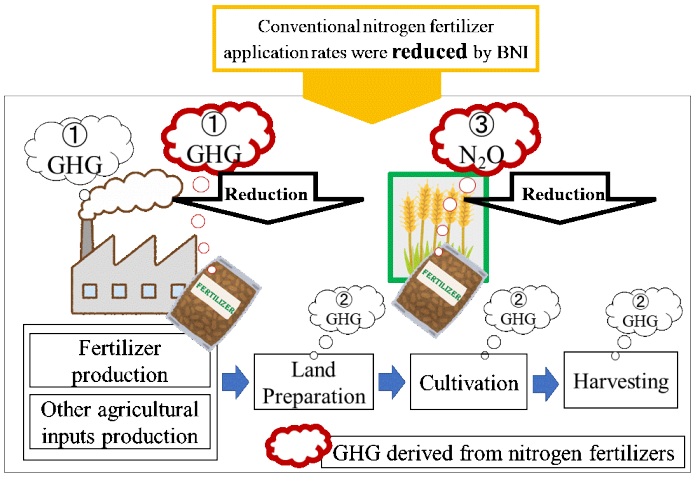

Fig. 1. Life Cycle Greenhouse Gas (GHG) emissions when nitrogen fertilizer-induced GHG emissions are reduced by BNI-enabled wheat

① GHG emissions from production of agricultural inputs such as fertilizer; ② GHG emissions from fuel consumption when machinery is used for land preparation, cultivation, and harvesting; ③ N_2O emissions from nitrogen fertilization applied in a field; and the sum of ①, ② and ③ is called "Life cycle greenhouse gas emissions." Nitrogen fertilizer-induced GHG emissions (GHG emissions from nitrogen fertilizer production and N_2O emissions from nitrogen fertilization, marked in red in Fig. 1) are reduced when nitrogen fertilizer application is reduced by BNI-enabled wheat.

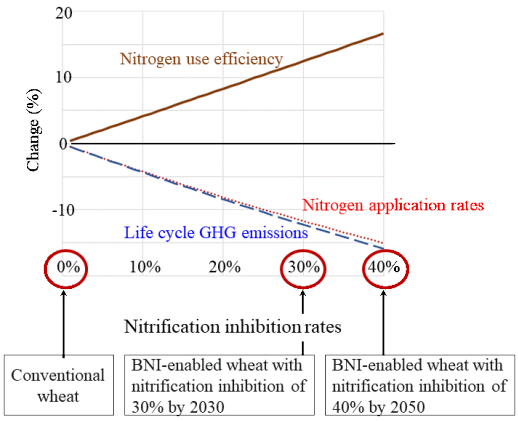

Fig. 2. Changes in life cycle GHG emissions, nitrogen fertilizer application rates, nitrogen-use efficiency, and nitrification inhibition rates caused by introduction of BNI-enabled wheat

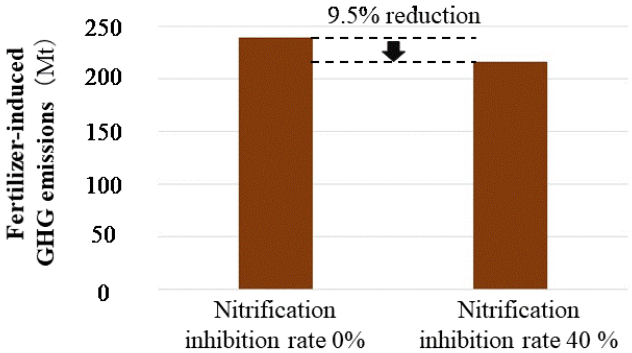

Fig. 3. Reduction in nitrogen fertilizer-induced GHG emissions when BNI-enabled wheat is introduced only to the area suitable for BNI-enabled wheat

Reference: Leon et al. (2022) *Environmental Science and Pollution Research* 29: 7153–7169. https://doi.org/10.1007/s11356-021-16132-2

Relationship between leaf and stem growths of a tropical timber tree, *Shorea leprosula*, in the family Dipterocarpaceae

Dipterocarpaceae is an important timber family in Southeast Asia. Dipterocarp species flower at irregular intervals from three to ten years, hindering the collection of seeds and provision of good planting materials. Furthermore, there is an urgent need to understand the effects of climate change on the production of these timber

species. Because stem elongation is a basis for seedling growth and timber production, it is important to elucidate how stem elongation is regulated in dipterocarps to solve these problems. However, the regulation of stem elongation is still not clear yet in dipterocarps.

To reveal it, we studied the regulation of stem elongation by focusing on the relationship between stem elongation and leaf growth. Through weekly observations of *S. leprosula* branches, we found that the branches have two clear growth phases, the active growth and the growth-arrested phases (Fig. 1). Although it has been discussed that branches of dipterocarps grow continuously or intermittently, this result indicates intermittent branch growths in *S. leprosula*. During the active growth phase, stems and young leaves coordinately grew (Fig. 1). Young leaves rapidly grew and were unfolded when stems showed clear elongations. Furthermore, internodes became significantly shorter if a young growing leaf was removed from the internodes (Fig. 2), suggesting that growing leaves positively regulate internode elongation.

Our previous study showed that small changes in ambient temperature regulate the timing of leaf growth in dipterocarps (Research Highlights 2020, C07). Thus, the observed regulation of stem growth by leaves would suggest that temperature changes also affect the timing of stem growth in *S. leprosula*. Considering the effect of temperature on stem growth in dipterocarps, our results will contribute to a stable supply of planting materials by controlling the growth of dipterocarp seedlings using multiple nurseries in different temperature conditions. Besides, we will be able to use the relationship between temperature and stem growth observed in this study when evaluating the effects of global warming on sustainable timber production of dipterocarps. Furthermore, because the removal of young growing leaves suppresses stem growth, damages on growing leaves could negatively affect the stem growth in dipterocarps. If climate change increases the damage on young leaves by insect attacks and droughts, these damages will have negative impacts on seedling growth and timber production of dipterocarps. Further studies are required to evaluate more precisely these negative effects on dipterocarp forestry.

(M.J. Kobayashi, N. Tani, K.K.S. Ng [Forest Research Institute Malaysia (FRIM)], S.L. Lee [FRIM], N. Muhammad [FRIM])

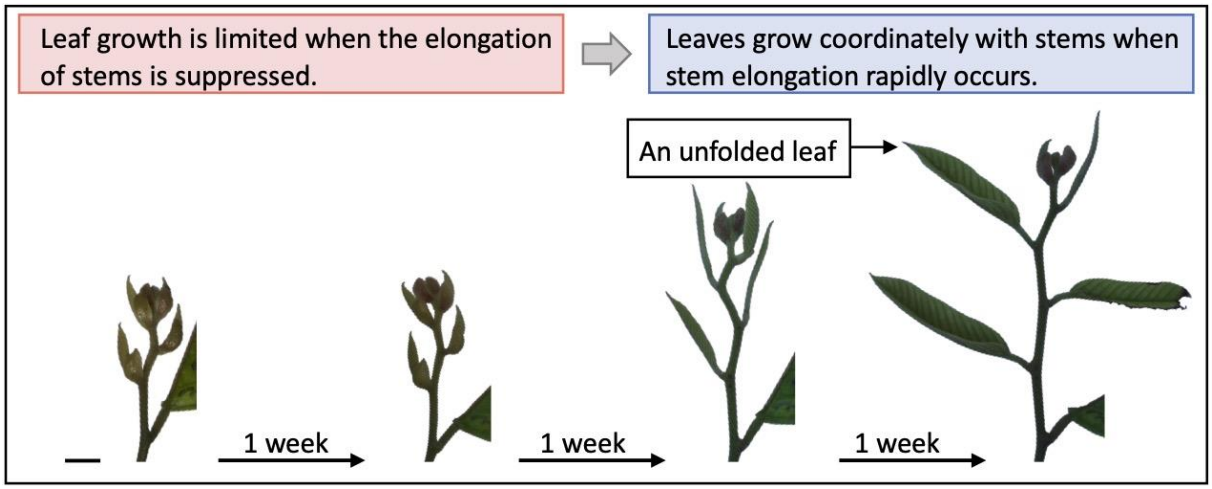

Fig. 1. The leaf and stem growths on an intermittently growing *S. leprosula* branch
The figure shows the result of weekly observation of an *S. leprosula* branch. As shown in the two pictures on the left, *S. leprosula* branches show a growth-arrested phase for several weeks. However, during an active growth phase as shown in the two pictures on the right, the rapid growth of branches is observed. Due to the active growth and growth-arrested phases, *S. leprosula* branches grow intermittently. Leaves and stems coordinately grow on *S. leprosula* branches. Young leaves rapidly grow and are unfolded when stems show clear elongations. Scale bar indicates 1 cm.

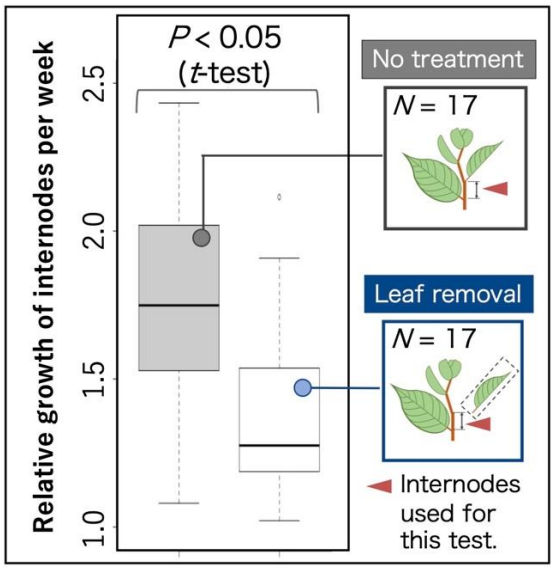

Fig. 2. The effect of growing leaves on the internode growths of *S. leprosula*
The relative growths of the internodes whose growing leaves were experimentally removed (right) were significantly smaller than those of the control (left). The red arrowhead indicates the position of internodes measured to test the changes in growth rate. N represents the number of branches used for the experiment.

Reference : Kobayashi et al. (2021) *JARQ* 55(3):273–283

Teak growth doubles in the Lao Mountains depending on the control of stand density and topographic conditions

Teak plantations are being promoted in the mountainous areas of Lao PDR including in Luang Prabang Province. However, teak growth varies greatly depending on the conditions of the planting site. Clarification of the factors related to the growth of planted teak and establishment of a suitable land determination method will be the basis of effective land use in mountainous areas.

In this study, the growth history of teak trees was estimated from annual rings for each of the three canopy trees felled from 27 plots of teak plantations aged 20 and over in the southwestern part of Luang Prabang Province. A total of 81 teak trees were felled and cut into round slices at regular intervals to create a disk, and the annual rings were read. Based on the analysis of annual rings, we estimated the diameter growth and tree height growth process of each teak tree with the age and analyzed the relationship between tree growth and topographic conditions as well as stand density.

The diameter growth (Fig. 1, left) and tree height growth (Fig. 1, right) of planted teak differ by about twice.

The diameter growth and tree height growth of teak individuals are significantly affected by the shape and gradient of the slope to be planted (Fig. 2). For the fast growth of teak, the gradient of slope should be gentle, with the concave part considered better than the convex part and the lower part deemed better than the upper part of the slope.

In the study area, the actual stand density of planted teak was about 500 to 1,600 trees/ha at the stand age of 20 years and over. In that range, the lower the tree density, the better the diameter growth and tree height growth.

This teak suitability determination method can be disseminated to farmers by technical instructors because the index used can be obtained by simple measuring instruments or visual measurement at the site. Substituting the output of the prediction formulas for diameter growth and tree height growth into the volume estimation formula leads to the prediction of teak yield. This result is expected to be applied to areas with similar climate, meteorology, geology, and soil conditions (for example, northern Thailand) with some correction.

(A. Imaya [Forestry and Forest Products Research Institute],
S. Vongkhamho [Forestry Research Center, NAFRI, Lao PDR],
C. Takenaka [University of Nagoya], K. Yamamoto [University of Nagoya],
H. Yamamoto [University of Nagoya])

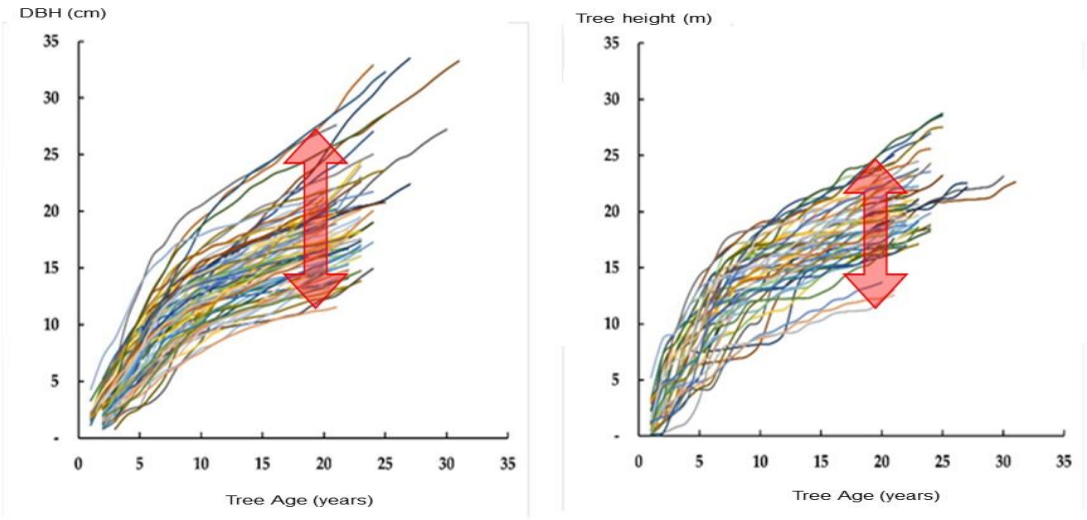

Fig. 1. Diameter growth (left) and height growth (right) of planted teak

Note: Growth history was estimated from annual rings for each of the three canopy trees felled from 27 plots of teak plantations.

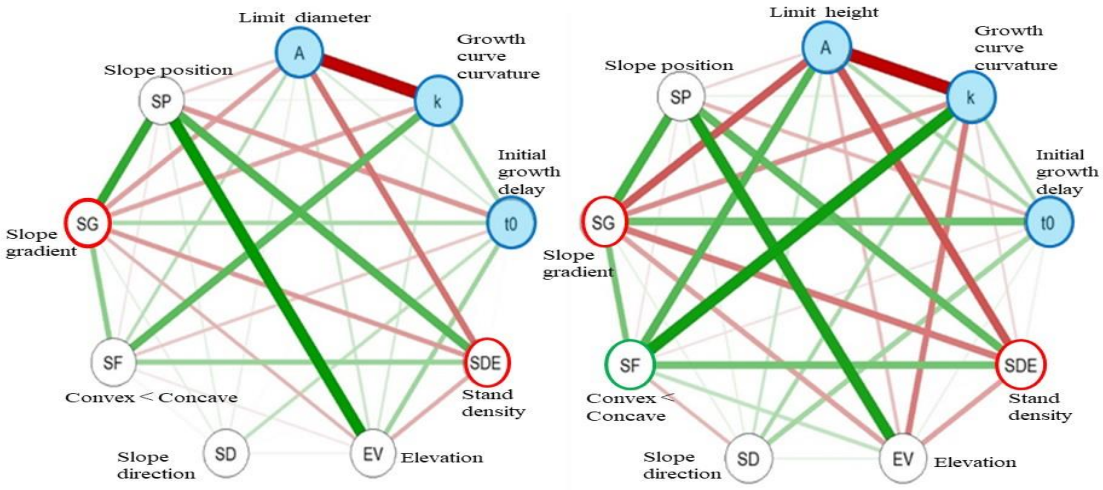

Fig. 2. Partial correlation network between DBH–age growth curve parameters and topographic conditions (left) and height–age growth curve parameters and topographic conditions (right)

Note: The green and red lines indicate positive and negative correlations, respectively. The line thickness indicates the strength of the Spearman's partial rank correlation. The letters in blue circles indicate variables of tree growth parameters A, k, t_0 in Mitscherlich growth function; $Y=A(1-\exp(-k(t_i-t_0))$. Other circles indicate stand density (SDE) and topographic conditions such as elevation (EV), slope gradient (SG), slope direction (SD; N<E<S<W), slope form (SF; convex<concave) and slope position (SP). The factors in green circle ○ and red circle ○ have significant positive and negative relationships with growth at the 1% level.

Reference: Vongkhamho et al. (2022) *Forests* 13, 118. https://doi.org/10.3390/ f13010118

Figures reprinted/modified with permission.

Calculation of rice farmers' premiums for index-based flood insurance

There is concern that climate change will induce extreme events such as severe droughts, high tides, and bigger cyclones. Thus, the development of non-life insurances products targeting crops is desired in the Ayeyarwady region in Myanmar, where cyclone Nargis caused severe damage in 2008. The development of weather index insurance is progressing because it does not require actual surveys of damaged areas, and farmers do not abandon cultivated areas impacted by a disaster. However, it is difficult for farmers to understand what crop insurance is and to calculate the insurance money needed to maintain farming operations. Therefore, this research aimed to provide a method to calculate the optimum insurance money for farmers.

An insurance money function is derived by solving a utility maximization problem, taking into account the receipt of insurance money and premium payments for a risk averse farmer. The insurance money and the premium are found by substituting the average numbers of the 320-farm data (Table 1). These are shown to correspond to the farm price of rice and risk aversion rate of the farmer. If the relative risk aversion rate is zero, plus, and minus, the farmers are risk neutral, risk averter, and risk lover, respectively. If the farm price of rice goes up from 280 to 320 Kyat per kg, the annual premium that an average farmer with an average cropping area of 5.6 ha willingly pays will increase from 10,000 to 120,000 Kyat (Fig. 1). If the relative risk aversion rate rises from 0.1 to 0.9, the required insurance money will increase from 30,000 to 800,000 Kyat per average farmer (Fig. 2). If total rainfall from May to October is 3,700 mm which is the regional average; if the relative risk aversion rate is 0.68 which is the average number in Ethiopia in a previous research; and if the farm price of rice is 306 Kyat per kg which is the regional average, the premium will be 58,000 Kyat, i.e., around 42.6 USD per average farm. This calculated premium is equivalent to 3% of the average farm income.

Weather index insurance premiums can be calculated in response to changes in rainfall, relative risk aversion rate, farm price of rice, and input prices such as fertilizer price. The target disaster is flood. Flood disaster area rate during a period and marginal disaster area rate, which shows the rate of increase in disaster damage for 1 mm increase in rainfall, are required for application of the method to other regions.

(J. Furuya, A. Hirano,
S.S. Mar [Yezin Agricultural University], T. Sakurai [University of Tokyo])

Table 1. Data for calculation of insurance money and premium (n=320)

Variable	Unit	Number
Flood damage area rate	%	0.929
Marginal damage area rate	%	0.00065
Rainfall (May-Oct. total)	mm	3,700
Threshold of rainfall	mm	3,500
Farm price of rice	Kyat/kg	306
Price of fertilizer	Kyat/kg	630
Wage rate	000Kyat/(man day)	2.5
Capital user price	000Kyat/tractor	1,007
Land rent	000Kyat/acre	2,500
Fertilizer application	kg	1,128
Labor input	man day	392.1
Capital input	Harvest fee 000Kyat	607.8
Land input	acre	13.77
Fertilizer cost share	dimensionless	0.165 (modified to.0.232)
Labor cost share	dimensionless	0.274 (modified to 0.386)
Capital cost share	dimensionless	0.167 (modified to 0.235)
Land rent share	dimensionless	0.104 (modified to 0.146)
Total of cost share	dimensionless	0.710 (modified to 1.000)
Relative risk aversion	dimensionless	0.68
Margin of non-life insurance company	%	0.1

Note: 1 US Dollar = 1,360 Kyat, 108.8 JPY, in 2016 (survey period average), Relative risk aversion data is from a previous research in another country.

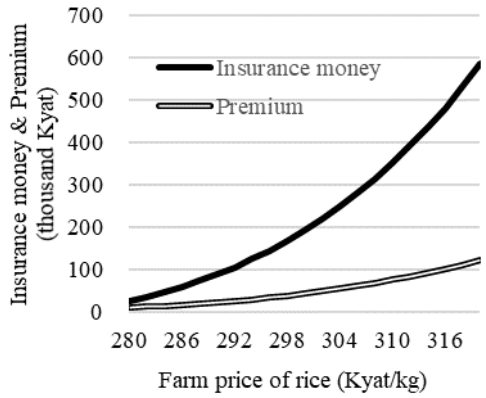

Fig. 1. Price of rice and premium
If the farm price of rice goes up, the demand for insurance will increase.

Note: Total rainfall from May to October is 3,700 mm, relative risk aversion is 0.68.

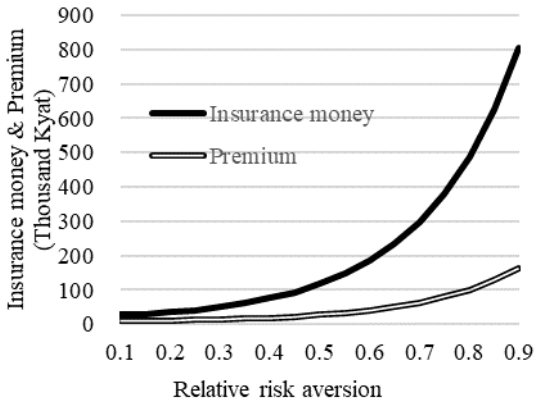

Fig. 2. Risk aversion rate and premium
If the risk aversion rate is close to 1.0, the required insurance money will increase significantly.
Note: Total rainfall from May to October is 3,700 mm, price of rice is 306 Kyat/kg.

Reference: Furuya et al. (2021) *Paddy and Water Environment* 19: 319–330. https://doi.org/10.1007/s10333-021-00859-2

African phosphorus fertilizer from indigenous low-grade phosphate rock could replace imported phosphorus fertilizer in rain-fed rice cultivation

In tropical semi-arid regions including Burkina Faso, soils with low phosphorus (P) availability are widely distributed, limiting rainfed rice production. Fertilizer application rates by local farmers are limited mainly due to the high price of imported P fertilizers. A vast amount of phosphate rock deposits are found in Africa. However, most of them have been rarely utilized because of the high impurity and low solubility. If local P fertilizer can be manufactured from this unused resource, it is expected to reduce fertilizer prices and increase fertilizer application rate. Japan International Research Center for Agricultural Science (JIRCAS) has succeeded in increasing the solubility of low-grade African phosphate rock by applying two major methods: partial acidulation and calcination. Imported superphosphate (SSP) mostly consists of water-soluble P (Table 1). On the other hand, partially acidulated phosphate rock (PAPR) consists of water-soluble P and ammonium citrate-soluble P, and calcinated phosphate rock (CPR) of ammonium citrate-soluble P and citric acid-soluble P (Table 1). The solubility is in the order of water-soluble P > ammonium citrate-soluble P > citric acid-soluble P. A field experiment was conducted on the river bottom, which is the main area for rainfed rice cultivation, and on the riverside slope where rainfed rice cultivation can be expanded (Fig. 1, upper panel) to identify the effect of African P fertilizer on rice grain yield.

Rice grain yield is significantly increased by SSP application at all sites on the river bottom and riverside slope (Fig. 1, middle panel), suggesting that P is a limiting factor in rice cultivation. In the river bottom, both partially acidulated and calcined phosphate rock show comparable performance with SSP (Fig. 1, lower panel). Therefore, both can replace imported P fertilizer. In the lower and middle parts of the riverside slope, partially acidulated phosphate rock is as effective as SSP, while calcined phosphate rock is not (Fig. 1, lower panel). Both water-soluble and ammonium citrate-soluble P contributed to grain yield in the river bottom with a high ground-water level, and only water-soluble P contributed to grain yield on the riverside slope with a low ground-water level (Table 2). Therefore, the differences in fertilization effect can be explained by the differences in P composition in fertilizer (Table 1).

Partially acidulated and calcined phosphate rock fertilizers from African low-grade phosphate rock can be widely used in rain-fed rice cultivation in tropical semi-arid regions. Information on effective P fraction in rainfed rice cultivation will be useful for developing the locally adopted P fertilizer.

(S. Iwasaki, K. Ikazaki, S. Nakamura, F. Nagumo,
M. Fukuda [National Agriculture and Food Research Organization],
K. Ouattara [Institute of the Environment and Agricultural Research, Burkina Faso])

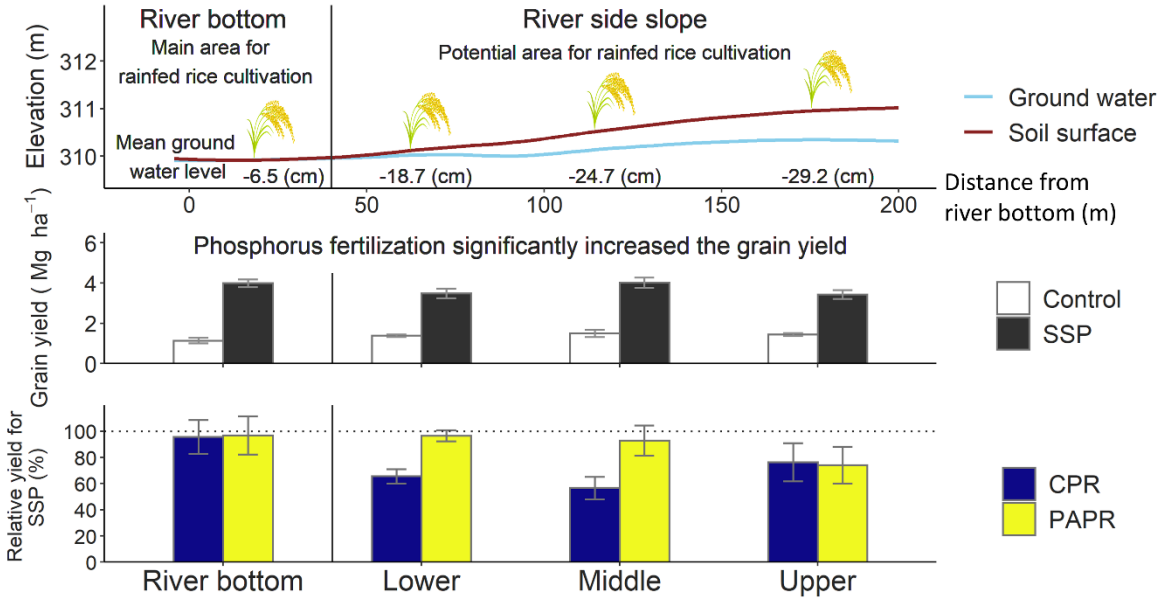

Fig. 1. Outline of the field experiment and fertilization effect of African phosphorus fertilizer from low-grade phosphate rock

Error bar: standard error

Table 1. Phosphorus composition of fertilizers

Types of phosphorus fertilizers	Phosphorus composition High ← Solubility ← Low Water-soluble phosphorus	Ammonium citrate-soluble phosphorus	Citric acid-soluble phosphorus
Single superphosphate (Imported phosphorus fertilizer)	◎	×	×
Partially acidulated phosphate rock	○	○	×
Calcinated phosphate rock	×	○	◎

◎ : > 50%, ○ : 25–50%, ×: < 25%

Table 2. Contribution of phosphorus fraction to the yield

Phosphorus composition	River bottom	Riverside slope		
		Lower	Middle	Upper
Water-soluble phosphorus	◎	◎	◎	◎
Ammonium citrate-soluble phosphorus	◎	○	△	×
Citric acid-soluble phosphorus	×	×	×	×

◎: contributes at 1% level, ○: contributes at 5% level, △: contributes at 10% level

Reference: Iwasaki S et al. 2021. *Soil Science and Plant Nutrition*, 67 (4), 460–470.
https://doi.org/10.1080/00380768.2021.1932584

Identification and validation of a major QTL for primary root length in soybean

The root system absorbs water and nutrients, which are essential for plant growth, from the soil. The phenomenal formation of a robust and extensive root system is extremely important in crop plants because it ensures their adaptability to the surrounding environment and their improved resource acquisition in the low input environment. However, roots are the hidden part of plants and have high adaptive plasticity in various environments. Therefore, the characterization of the root system requires considerable efforts in field conditions. The large variation observed in root traits suggested that the improvement of soybean by the genetic alteration of root traits is feasible. In this study, genetic analysis was conducted with an aim to identify quantitative trait loci (QTL) associated with primary root length (PRL) in soybean.

A total of 103 F_7 recombinant inbred lines (RILs) derived from a cross between “K099” (short primary root) and “Fendou 16” (long primary root) were used to identify QTL for PRL. “Fendou 16” is a soybean cultivar from Shanxi, China, and “K099” is a Korean soybean cultivar. Linkage groups were constructed with 223 simple sequence repeat markers from the 20 chromosomes. Phenotyping for PRL was performed in hydroponic conditions. QTL analysis identified a major QTL (*qRL16.1*) on chromosome 16 between SSR markers Sat_165 and Satt621, explaining 30.25% of the total phenotypic variation (Fig. 1). The effect of *qRL16.1* was confirmed using *qRL16.1* near-isogenic lines (NILs). PRL was significantly longer in NILs possessing the *qRL16.1* allele of “Fendou 16” compared to allele of “K099” (Fig. 2). In addition, to validate *qRL16.1* in a different genetic background, QTL analysis was performed in another F_6 RIL population derived from a cross between “Union” (medium primary root) and “Fendou 16,” in which a major QTL was detected again in the same genomic region as *qRL16.1*, explaining 14% of the total phenotypic variation for PRL.

qRL16.1 is a novel QTL for primary root length in soybean which provides important information for understanding the genetic control of root development. Identification of this major QTL will facilitate positional cloning and DNA marker-assisted selection for improvement of root traits in soybean.

(D. Xu, H. Chen [Jiangsu Academy of Agricultural Sciences, P.R. China], K. Giriraj [ICAR-Indian Institute of Soybean Research, India], Y. Yan [Xinjiang Academy of Agricultural Sciences, P. R. China.], B. Fan [Hebei Academy of Agricultural and Forestry Sciences, P. R. China)

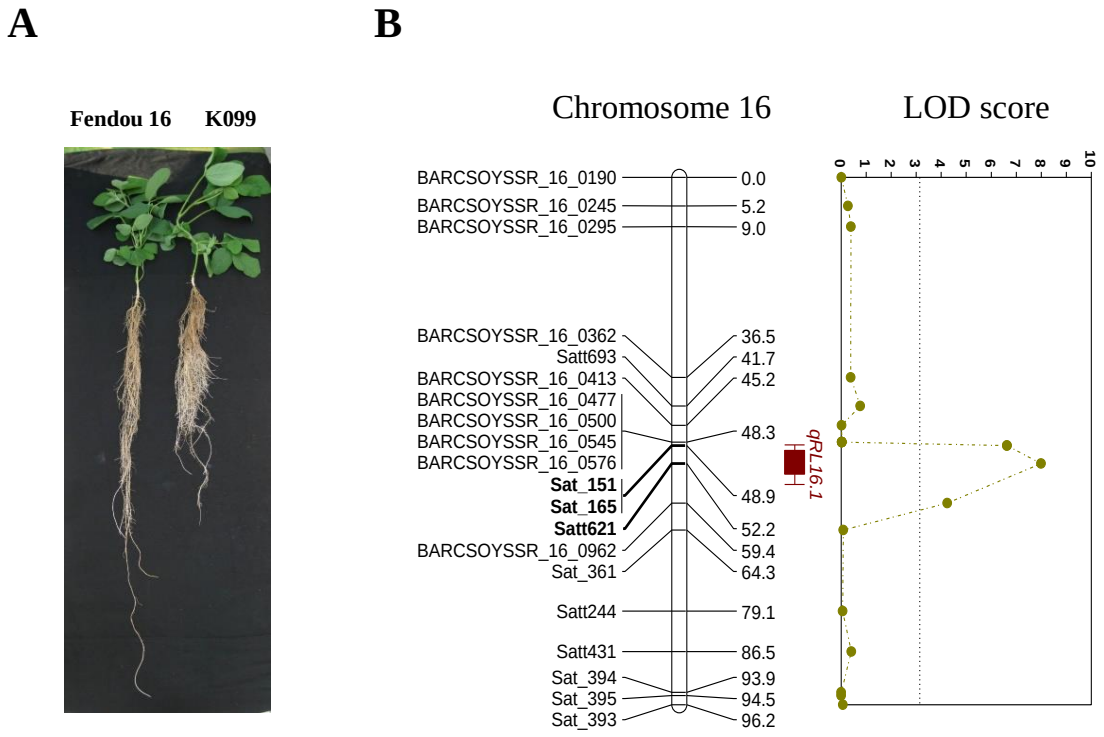

Fig. 1. The primary root length QTL (*qRL16.1*) detected on chromosome 16 in the RIL population derived from a cross between "K099" and "Fendou 16"

(A) Comparison of root architecture between "Fendou 16" and "K099" grown in hydroponic conditions. (B) Position and LOD score of the primary root length QTL (*qRL16.1*).

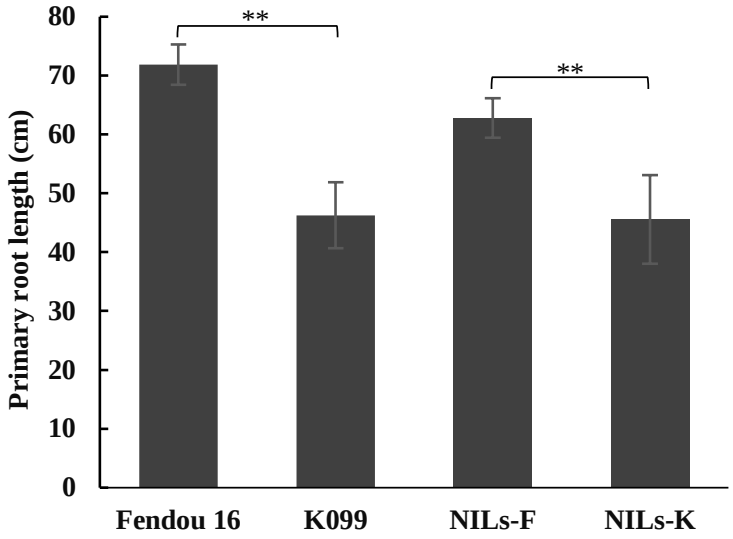

Fig. 2. Effect of the *qRL16.1* allele on primary root length of two near isogenic lines, NILs-F and NILs-K

NILs-F: "Fendou 16" genotype; NILs-K: "K099" genotype. Error bars indicate SD (n = 8).
**: $P < 0.01$.

Reference: Chen et al. (2021) *BMC Genomics*, 22:132. https://doi.org/10.1186/s12864-021-07445-0
Figures reprinted/modified with permission.

A major and stable quantitative trait locus *qSS2* for seed size and shape traits in soybean

Soybean [*Glycine max* (L.) Merr.] is one of the world's most economically important food and oil crop. It is a rich source of edible oil and protein, and provides substrate for several important food products. Seed size traits such as length, width, thickness, and single seed weight, and seed shape traits such as length-to-width, length-to-thickness and width-to-thickness, are important determinants of seed yield and appearance quality in soybean. Understanding the genetic architecture of these traits is important to enable their genetic improvement through efficient and targeted molecular breeding by design in soybean, and for the identification of underlying causal genes.

To identify quantitative trait locus (QTL) controlling seed size and shape traits in soybean, a recombinant inbred line (RIL) population developed from K099 (small seed size) × Fendou 16 (large seed size) was phenotyped in three growing seasons (2012, 2016, and 2017) in field conditions. A genetic map of the RIL population was developed using 1,485 genotyping by random amplicon sequencing-direct (GRASDi) and 177 SSR markers. QTL analysis was conducted using the QTL IciMapping software. As a result, a total of 53 significant QTLs for seed size traits and 27 significant QTLs for seed shape traits were identified. Six of these QTLs (*qSW8.1*, *qSW16.1*, *qSLW2.1*, *qSLT2.1*, *qSWT1.2*, and *qSWT4.3*) were identified with LOD scores of 3.80–14.0 and R^2 of 2.36%–39.49% in at least two growing seasons. Among the above significant QTLs, 24 QTLs were grouped into 11 QTL clusters, with three major QTLs (*qSL2.3*, *qSLW2.1*, and *qSLT2.1*) clustered into a major QTL on chromosome 2, named as *qSS2*. The effect of *qSS2* was validated in a pair of near isogenic lines, and its candidate genes (*Glyma.02G269400*, *Glyma.02G272100*, *Glyma.02G274900*, *Glyma.02G277200*, and *Glyma.02G277600*) were mined.

The identified QTLs will pave the way for positional cloning of genes regulating seed size and shape traits and for further understanding of their molecular mechanism in soybean. The results of this study will assist in breeding programs aimed at improving seed size and shape traits in soybean.

(D. Xu, H. Chen [Jiangsu Academy of Agricultural Sciences, P.R. China], K. Giriraj [ICAR-Indian Institute of Soybean Research, India])

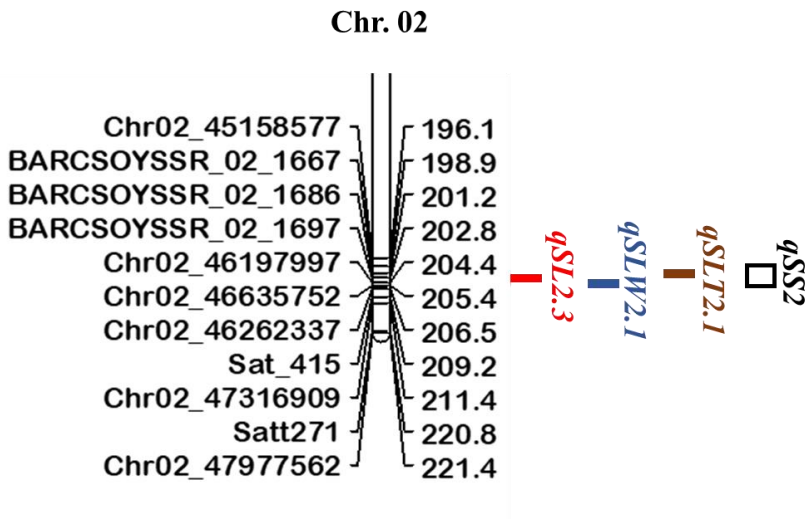

Fig. 1. Map position of a QTL cluster (*qSS2*) for seed size and shape traits on chromosome 2 in the K099 × Fendou 16 RIL population

Distances in cM are indicated to the right of the linkage groups and names of markers are shown on the left. *qSL2.3*, *qSLW2.1*, and *qSLT2.1* represent QTLs for seed length, length-to-width, and length-to-thickness, respectively.

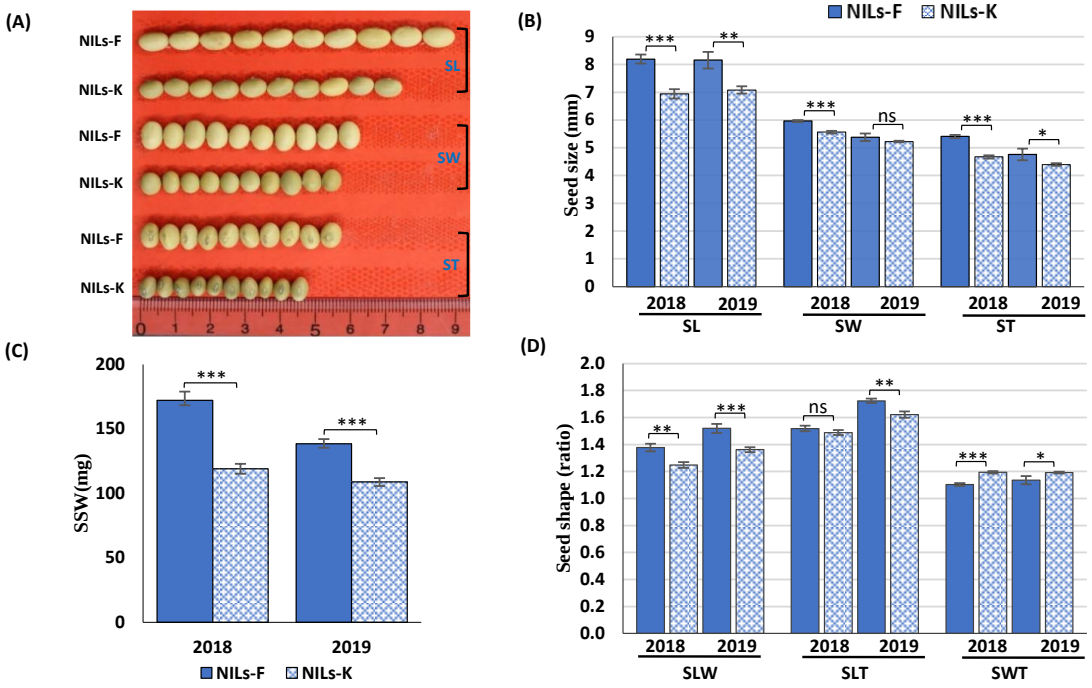

Fig. 2. Seed size and shape phenotypes of near isogenic lines, NILs-F and NILs-K, in 2018 and 2019. (A) phenotypic appearance, (B) SL, seed length; SW, seed width; ST, seed thickness, (C) single seed weight (SSW), and (D) seed shape traits (SLW, ratios of seed length-to-width; SLT, seed length-to-thickness; and SWT, seed width-to-thickness)

Error bars represent means ± SD of three replicates. Asterisks indicate significant differences between NILs-F and NILs-K at 5% (*), 1% (**), and 0.1% (***); ns indicates no significant difference at the 5% level in Student's *t*-test.

Reference: Kumawat and Xu (2021) *Frontiers in Genetics*, 12:646102. https://doi.org/10.3389/fgene.2021.646102

Functional analysis of genes in quinoa using a virus vector system

Quinoa (*Chenopodium quinoa* Willd.) is an annual protein-rich pseudocereal native to the Andean region of South America. Quinoa has been recognized as a potentially important crop in terms of global food and nutrition security since it can thrive in harsh environments and has an excellent nutritional profile. JIRCAS and collaborative researchers have been analyzing the complex and heterogeneous allotetraploid genome of quinoa, and have recently overcome the challenges, with the whole genome-sequencing of quinoa and the creation of genotyped inbred lines (Research Highlights 2016, B03: Draft genome sequence of an inbred line of *Chenopodium quinoa*, an allotetraploid pseudocereal crop with high nutritional properties and tolerance to abiotic stresses; Research Highlights 2020, B08: Genetic and phenotypic variation of agronomic traits and salt tolerance among quinoa inbred lines). However, the lack of technology to analyze gene function *in planta* is a major limiting factor in quinoa research.

In this study, we demonstrate that the virus-mediated transient gene expression or repression techniques can be used in quinoa plants (Fig. 1). We show that apple latent spherical virus (ALSV) vector can induce gene silencing of a quinoa carotenoid biosynthesis gene, phytoene desaturase (*CqPDS1*) (Fig. 2). Virus-mediated silencing of *CqPDS1* induces decreased accumulation of carotenoids and causes photobleaching symptoms in quinoa plants (Fig. 3). We also show that ALSV-mediated gene silencing can also be used in a broad range of quinoa inbred lines derived from the northern and southern highland and lowland sub-populations. Our data also indicate that repression of a quinoa 3,4-dihydroxyphenylalanine 4,5-dioxygenase gene (*CqDODA1*) or a cytochrome P450 enzyme gene (*CqCYP76AD1*) reduces accumulation of red-violet betalain pigments in quinoa plants (Fig. 4).

Our data demonstrate that the virus vector system is a useful tool for evaluating gene function in quinoa, where molecular breeding techniques such as genetic transformation have not been developed yet. Functional validation of quinoa genes, utilizing the published genomic information, could provide gene resources for molecular breeding of quinoa.

(T. Ogata, M. Toyoshima, C. Yamamizo-Oda, Y. Kobayashi, K. Fujii, Y. Nagatoshi, Y. Fujita, K. Tanaka [Actree Corporation], T. Tanaka [Actree Corporation], H. Mizukoshi [Actree Corporation], Y. Yasui [Kyoto University], N. Yoshikawa [Iwate University])

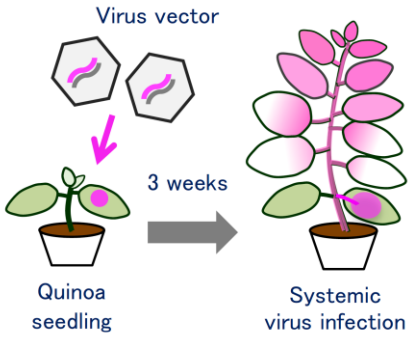

Fig. 1. Schematic of the virus vector system in quinoa plants

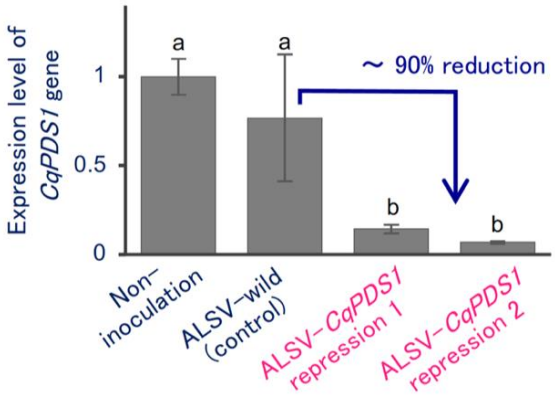

Fig. 2. ALSV induces silencing of carotenoid biosynthesis genes *CqPDS1* in quinoa.
RT-qPCR quantification of *CqPDS1* transcripts in the uninoculated upper leaves of plants inoculated with the indicated inocula. Data are normalized and are shown as means ± SD ($n = 3$). Different letters indicate significant differences ($p < 0.05$).

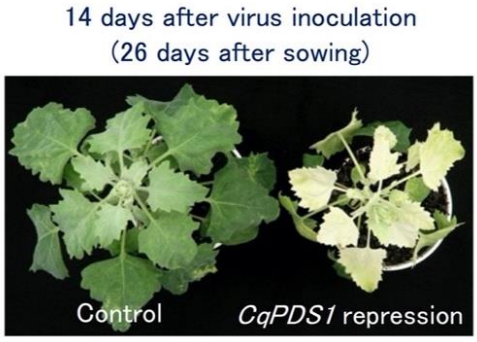

Fig. 3. Silencing of *CqPDS1* induces photobleaching phenotypes in quinoa plants.
A representative image of quinoa plants (inbred Iw line) at 14 days after virus inoculation with ALSV-wild (control) and ALSV-CqPDS1 is shown.

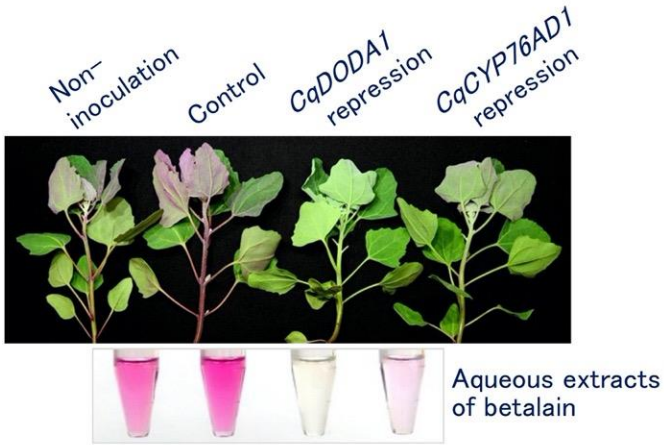

Fig. 4. Functional analysis of genes for betalain pigments biosynthesis in quinoa using the virus vector system
Virus-mediated silencing of *CqDODA1* and *CqCYP76AD1* inhibits betalain production in quinoa. Representative images of quinoa plants (inbred J056 lines) and aqueous extracts from the uninoculated upper leaves are shown. Quinoa plants inoculated with ALSV-wild were used as a control.

Reference: Ogata et al. (2021) *Frontiers in Plant Science* 12: 643499

Genome sequence of the soybean fungal pathogen, *Cercospora kikuchii*

Diseases caused by *Cercospora* spp. are threats to soybean production in South American countries such as Argentina. *Cercospora kikuchii* (Tak. Matsumoto & Tomoy.) M. W. Gardner is a pathogen of Cercospora leaf blight and purple seed stain in soybean. The symptoms appear on several parts of soybean plant, for instance, leaves, petioles, and seeds. Fungicide is one of the main management methods against this devastating disease. However, it was reported that some agrochemicals are losing effectiveness against the pathogen. High-quality genomic information of *C. kikuchii* can provide fundamental insights toward understanding the disease, and such studies will contribute to designing a molecular diagnosis method for the disease.

We selected the *C. kikuchii* isolate MAFF 305040 for this research. This was isolated in Japan and deposited to the Genebank of the National Agriculture and Food Research Organization (Tsukuba, Ibaraki, Japan). Sufficient depth of genome sequencing generated a high-quality genome assembly of this pathogen. The final genome assembly contained nine contigs comprising 34.44 Mb (Table 1, Fig. 1). The number of genes predicted from the genome assembly was 13,001 (Table 1). Completeness of the dataset was estimated using BUSCO (Table 1). From the predicted coding sequences, candidates for pathogenicity-related genes, namely, effector genes, secondary metabolite gene clusters, and genes of carbohydrate-active enzymes (CAZymes) were selected (Fig. 1).

The genome sequence was deposited in public databases (Table 1). The data can be used as a source in *C. kikuchii* genomic studies. Coding regions and functions of encoding proteins in this genome sequence should be validated since these were predicted from the assembled genomic sequence based on the database of genes/proteins of other organisms.

(T. Kashiwa, T. Suzuki [Utsunomiya University])

Table 1. Description of the genome assembly

Features	Value
Isolate name	MAFF 305040
Assembly size (bp)	34,440,063
Number of contigs	9
Number of predicted genes	13,001
BUSCO completeness	99.4%
Accession number*	BOLY00000000

*DDBJ/EMBL/GenBank accession number

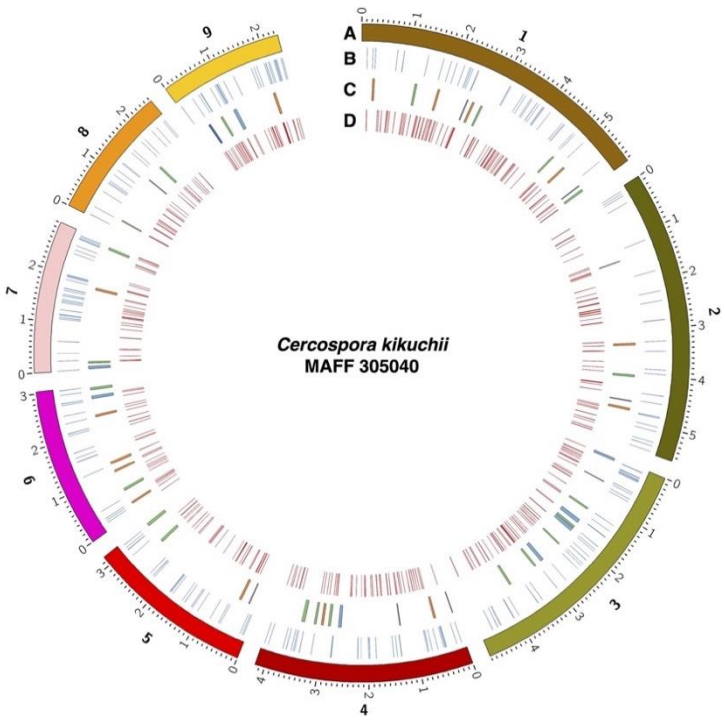

Fig. 1. Graphical summary of the genome assembly

Circos plot of the genome assembly. Track A indicates nine contigs of the genome assembly. Minor ticks indicate 0.1 Mb. Positions of the predicted pathogenicity-related genes, namely, effector candidates (B), secondary metabolite gene clusters (C), and CAZyme genes (D) are also shown.

Reference: Kashiwa T and Suzuki T (2021) *G3: Genes|Genomes|Genetics*, 11 (10), jkab277.
https://doi.org/10.1093/g3journal/jkab277

The pathogenicity of Asian soybean rust pathogen in Mexico can be grouped into two broad trends

Asian soybean rust (ASR) caused by *Phakopsora pachyrhizi* is the most important soybean disease in tropical and subtropical soybean cultivation areas. In Mexico, domestic soybean production is increasing each year, and with it, ASR disease has become a major problem. Plant disease control through the introduction of resistant varieties is advantageous in terms of low cost and low environmental impact, but resistance genes must be selected for breeding according to the virulence of the target pathogen. Thus, we analyzed the virulence of *P. pachyrhizi* populations in the major soybean production areas in Mexico.

ASR samples were taken from major soybean production areas in Mexico. Four samples were collected in Tamaulipas and San Luis Potosi states in 2015, and 19 samples were collected in Tamaulipas and Chiapas states from 2016 to 2019. These 23 samples were inoculated onto 12 ASR differential varieties and the reactions were evaluated as resistant, intermediate, or susceptible types. Clustering analysis showed that these ASR samples were classified into two groups (Group 1 and Group 2) that exhibited different virulence characteristics (Fig. 1A). Group 1 consisted of ASR samples collected from Tamaulipas, where soybean varieties carrying the resistance gene *Rpp1-b* were resistant and effective for disease control. However, soybean PI 200492 carrying *Rpp1*, PI 230970 carrying *Rpp2*, and PI 462312 carrying *Rpp3* showed susceptibility to ASR infection in most samples, thus the genes were not effective. (Figs. 1B and 1C). These characteristics were consistent with those exhibited by many of the ASR pathogens in South America. Group 2, on the other hand, consisted mainly of ASR samples collected from Chiapas. Five differential varieties with four resistance genes showed opposite reaction patterns to those from Tamaulipas. The virulence characteristics of this group were consistent with those reported for many ASR fungi in North America. It is rare to observe such clear geographic variation in virulence within a small area of a single country.

The present study found that Mexico has diverse ASR pathogen populations with the virulence characteristics of those reported from both South and North America. We also found a highly virulent ASR sample, MRP-16, which is pathogenic to all seven resistance genes except *Rpp1-b* of PI 587880A. The gene-pyramided line (No6-12-1) carrying the three resistance genes *Rpp2*, *Rpp4*, and *Rpp5* was resistant to all ASR samples, including MRP-16, and effective in controlling the disease (Fig. 1B). This gene-pyramided line, which is effective against Mexican ASR, is also known to show high resistance, making it a promising breeding material in Mexico. In addition, identifying factors that contribute to the large differences in virulence detected in this study may be helpful in ASR control.

(N. Yamanaka, J.C. García-Rodríguez [National Institute for Forestry, Agriculture and Livestock Research, Mexico])

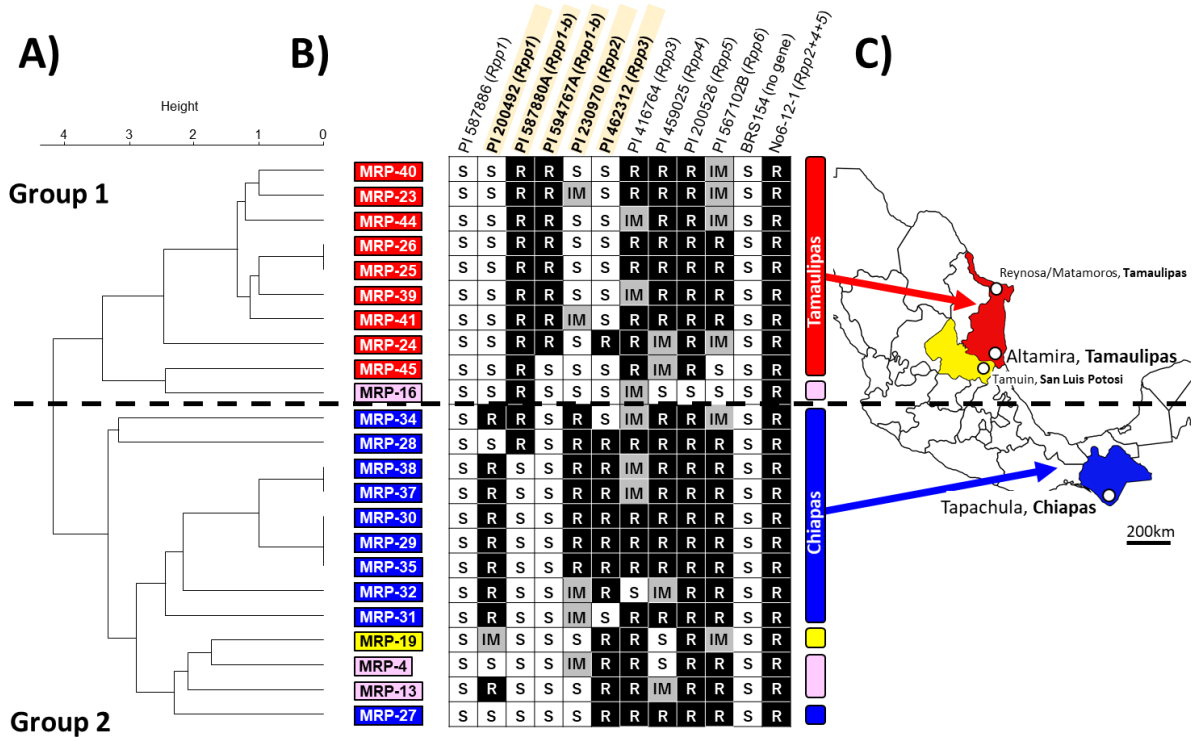

Fig. 1. A dendrogram of Asian soybean rust samples (MRPs) collected in Mexico based on their virulence (A), reaction profiles of the differential varieties (B), and regions where they were collected (C)

Samples obtained in 2016-2019 in Tamaulipas state are shown in red, samples obtained in 2015 in pink, samples obtained in 2015 in San Luis Potosi state in yellow, and samples obtained in 2018 in Chiapas state in blue. The parentheses after the name of the differential varieties indicate the resistance gene (*Rpp*) possessed by R, IM, and S for resistant, intermediate, and susceptible types, respectively.

References: García-Rodríguez et al. (2017) *Mexican Journal of Phytopathology*, 35(2):338–349. https://doi.org/10.18781/r.mex.fit.1701-5, and García-Rodríguez et al. (2021) *PhytoFrontiers*, 2(1): 52–59. https://doi.org/10.1094/PHYTOFR-06-21-0044-R

Gregarized desert locust females and males encounter just before oviposition in West Africa

Desert locusts are found in semi-arid regions from West Africa to India, and often cause serious agricultural damage. Since desert locusts are found in vast areas and adults in particular fly long distances, it is difficult to control them by spraying pesticides, and in order to mitigate the damage, it is necessary to develop control technologies based on desert locust ecology. To solve this problem, it is important to understand the behavioral patterns of desert locusts, especially how adult desert locusts mate and lay eggs in the field during the breeding season. Therefore, we conducted a field survey from 2011 to 2019 with the aim of elucidating the reproductive strategies of desert locusts in the Sahara Desert.

In this study, we conducted a field survey in the Sahara Desert, which stretches across Mauritania in West Africa, the habitat of desert locusts. We simultaneously recorded the sex ratio, mating status, and degree of ovarian development of a gregarized population. The results showed that the sex ratio of the population was skewed towards either sex. In the female-biased population, most of the female desert locusts were developing ovaries and were not mating, but most of the females in the male-biased population had large eggs that were about to be laid and were mating (Fig. 1). A closer look at the male-biased population revealed that during the daytime, gravid female desert locusts flew into the male group (Fig. 2) just before oviposition. After mating, the male remained on the female's back and continued their post-mating guarding (Fig. 3). In the evening, they gathered in the open sand near where they met, and we also found that they spawned in pairs at night (Fig. 3). It can be inferred that the male and female desert locusts are able to meet their partners efficiently while resolving sexual conflicts by living separately in groups. Pairs that are spawning in groups remain in place for several hours, making them good targets for pest control. If a group of male desert locusts is found, it is possible to reduce the amount of pesticides used by waiting for the group to spawn until nighttime instead of immediately controlling them.

As recommended by the Food and Agriculture Organization of the United Nations, intensive pesticide application timed to coincide with the identified periods of desert locust inactivity will lead to an environmentally and health-conscious pest control that does not use more pesticides than necessary.

(K.O. Maeno, P. Cyril [The French Agricultural Research Centre for International Development], S. Ould Ely [The Mauritanian National Anti-Locust Centre (CNLA)], M.E.H. Jaavar [CNLA], S. Ould Mohamed [CNLA], M.A. Ould Babah Ebbe [CNLA], S. Ghaout [The Moroccan National Anti-Locust Centre])

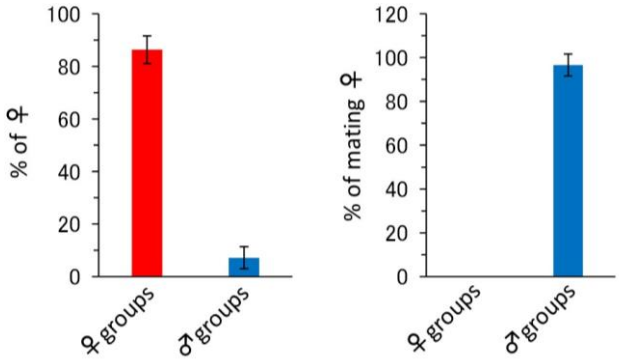

Fig. 1. Sex ratios and percentage of mating females of either groups of female- or male-biased sex ratios

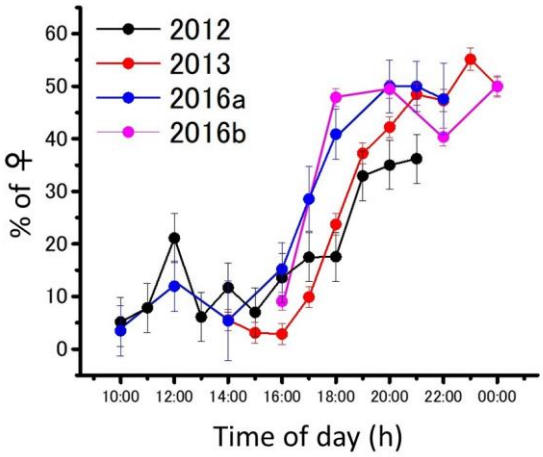

Fig. 2. Diel changes in the percentages of females in male-biased sex groups based on data from transect (2 m × 25 m)

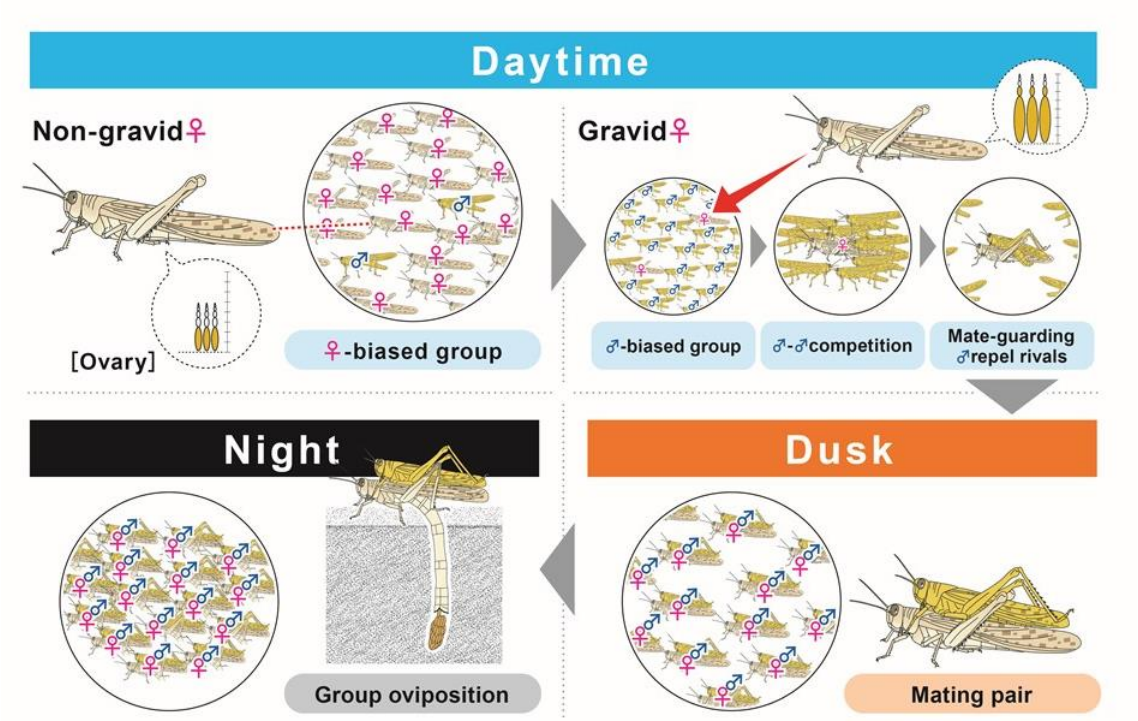

Fig. 3. During the day, female desert locusts with developing ovaries stay in groups with a skewed sex ratio toward females and do not mate. When females ready to lay eggs fly into a group of males, many males compete to mate. When one male rides on the back of the female, the other males give up, no further fighting occurs and then they mate. In the evening, they move in pairs to sandy areas suitable for oviposition and begin to aggregate. At night, they oviposit in groups.

Reference: Maeno et al. (2021) *PNAS*, 118 (42): e2104673118, https://doi.org/10.1073/pnas.2104673118

Predicting body growth and body mass index of farmed milkfish in the Philippines from water temperature

Information on the growth of farmed fish is important for aquaculture production planning and cost management. It also helps aquaculture managers understand the quality (fat content) and health status of farmed fish, including milkfish. Milkfish is the most important aquaculture target species in the Philippines. However, although milkfishes are actually raised in open-air conditions, only a few previous studies have focused on water temperature. Therefore, this study aimed to clarify the impact of changes in open-air water temperature on milkfish growth and body mass index.

A logistic model for growth (weight) of farmed milkfish was proposed as the most applicable statistical model, with data sampling conducted in high-temperature and low-temperature seasons (Fig. 1). In accordance with common fish farming practice, the experiment was conducted with satiated (full) feeding. The results show that the daily growth rate decreases as milkfish size increases (Fig. 2). The growth model also reflects these physiological characteristics. Regarding the relationship between body mass index and water temperature, body mass index (fat content) increases during low-temperature season (around 29－30°C) and decreases during high-temperature season (>30°C). The body mass index also decreases during the minimum temperature period (27－28°C) in low-temperature season (Fig. 3). As for the relationships among body mass index, water temperature, and feed conversion rate, feed conversion rate and body mass index decrease during high-temperature season. Conversely, they increase during low-temperature season (Fig. 4).

Previous studies have generally used linear regression analysis for estimating fish growth, which tended to exceed growth estimates up to the shipping size (300－400 g/fish). However, this model can be adjusted for such overestimates, and farm managers can utilize the model for more accurate growth and shipping forecasts. Based on the relationship between fish weight and growth rate, it is possible to predict the optimal size of fish to ship for efficient aquaculture business. However, because cost is not analyzed, it is not possible to estimate the optimal size for operating an aquaculture business from this research. Body mass index can be estimated from water temperature using the results; however, further data collection and model modification are needed to make more precise predictions. This research can provide insights for the amount of feed that should be fed at certain temperatures, for example, reducing the amount of feed during low-temperature season and keeping the level of fat constant throughout the year. Feeding cost represents the largest proportion of costs in fish aquaculture business, and the results of this research can contribute to guideline development and cost reduction.

(M. Kodama [Japan Fisheries Research and Education Agency], R. A. Diamante [Southeast Asian Fisheries Development Center (SEAFDEC)], N. Salayo [SEAFDEC], R. J. Castel [SEAFDEC], J. Sumbing [Yokohama National University])

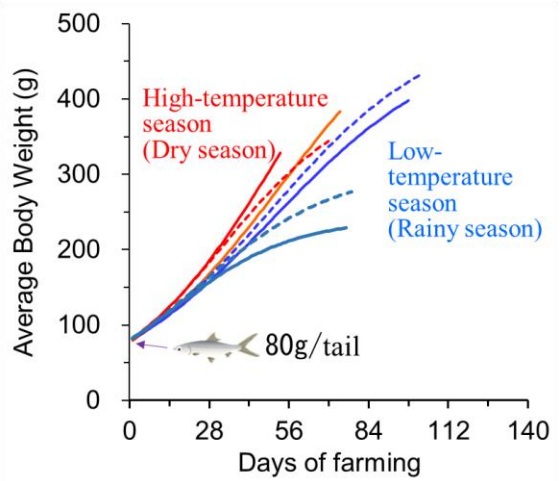

Fig. 1. Examples of weight growth estimation for different conditions as seasons

Solid and dashed lines are different farm facility locations. Experiments were conducted three times during the high-temperature season and four times during the low-temperature season. Starting with seedlings weighing 80 g/tail.

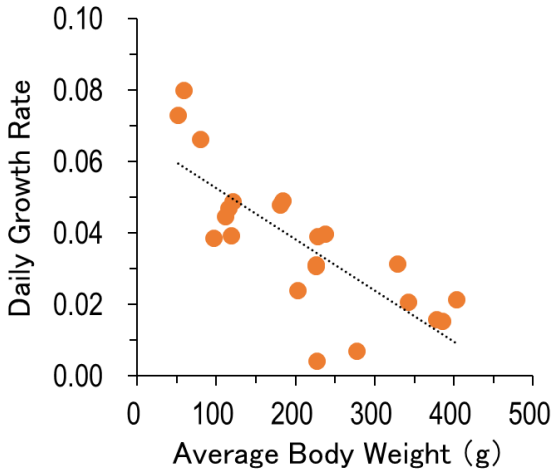

Fig. 2. Relationship between daily growth rate and fish weight

Daily growth rate = 100 × exp (((ln(Wf) –ln(Wi))/farming period) –1).

Wf is the weight at the time of measurement (g) and Wi is the weight at the beginning of farming (g).

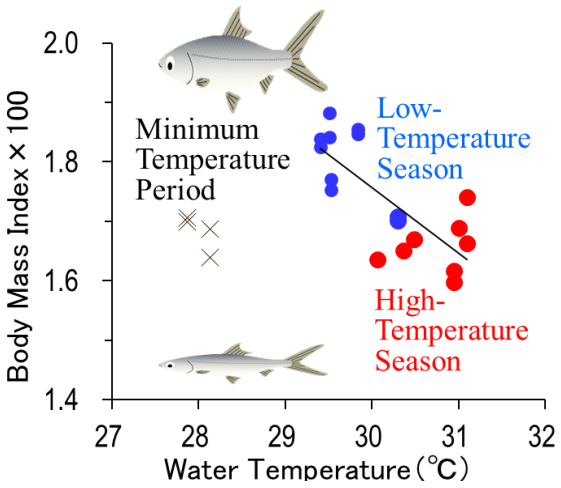

Fig. 3. Relationship between body mass index and water temperature

Body Mass Index = weight (g)/(length (cm))^2. Red dots correspond to BMI during high-temperature season, blue dots correspond to BMI during low-temperature season, and X marks indicate BMI during minimum temperature period.

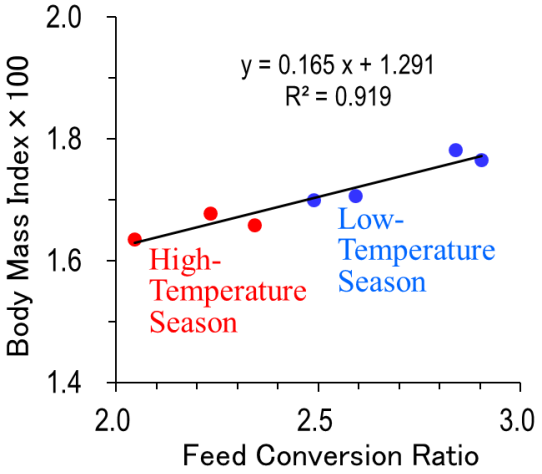

Fig. 4. Relationship between body mass index and feed conversion ratio

Feed conversion ratio = total feed consumed(g)/total weight of product produced(g). Data of the minimum temperature period are not included.

Reference: Kodama M et al. (2021) *JARQ* 55: 191−200, https://doi.org/10.6090/jarq.55.191

Germ cell cryopreservation to conserve genetic diversity in shrimps

Establishing sustainable aquaculture requires the development of techniques to prevent genetic deterioration of aquaculture populations and to produce superior strains such as disease-resistant strains. For this purpose, it is extremely important to preserve existing genetic diversity. In recent years, germ cell cryopreservation techniques and germ cell transplantation techniques for producing sperm, eggs, and larvae derived from cryopreserved germ cells have been developed for several fish species and are the only effective methods for preserving all genetic information in fish in which egg cryopreservation has not been available. However, such technology has not yet been developed for crustaceans, which are important species in fisheries. The only way to preserve genetic diversity of crustacean species is to keep a huge number of live individuals in aquariums or cages. To address this issue, this study will develop the first germ cell cryopreservation technique in crustacean for two species of prawns, the black tiger shrimp (*Penaeus monodon*) and banana shrimp (*Fenneropenaeus merguiensis*), both of which belong to Penaeidae.

In this study, we compared three commonly used cryoprotectants — dimethyl sulfoxide (DMSO), glycerol, and magnesium chloride ($MgCl_2$) — and found that 10% glycerol or 10% DMSO resulted in higher germ cell viability after cryopreservation in both species (Fig. 1). In terms of recovery rates, 10% glycerol and 10% DMSO resulted in higher recovery rates than other cryoprotectants in black tiger shrimp and banana shrimp, respectively (Fig. 2). Considering the survival and recovery rates together, it was concluded that 10% glycerol and 10% DMSO were suitable cryoprotectants for black tiger shrimp and banana shrimp, respectively. Furthermore, for both species, the vitrification method was found to be more suitable for long-term preservation than the slow-freezing method (Fig. 3).

Based on this study, the following are expected: 1) Since germ cells can be cryopreserved in liquid nitrogen storage containers, this technique will enable the preservation of genetic diversity of the black tiger shrimp and banana shrimp semipermanently without genetic deterioration and with less space and labor than rearing of live individuals; 2) cryopreservation of germ cells makes it possible to prevent genetic deterioration of aquaculture populations and to secure genetic breeding material which will be used in future breeding programs to produce superior strains before genetic diversity is lost, which can lead to sustainable shrimp aquaculture technology; and 3) based on this study, it is expected that germ cell cryopreservation techniques can be developed for other species of prawns, including many species with high economic value, to conserve the existing genetic diversity of these species. In addition to this study, if germ cell transplantation techniques are developed in crustaceans, it will also be possible to regenerate individuals from frozen germ cells.

(T. Okutsu, N. Rakbanjong [Prince of Songkhla University (PSU), Thailand], W. Chotigeat [PSU], A. Songnui [Department of Fisheries, Thailand], M. Wonglapsuwan [PSU])

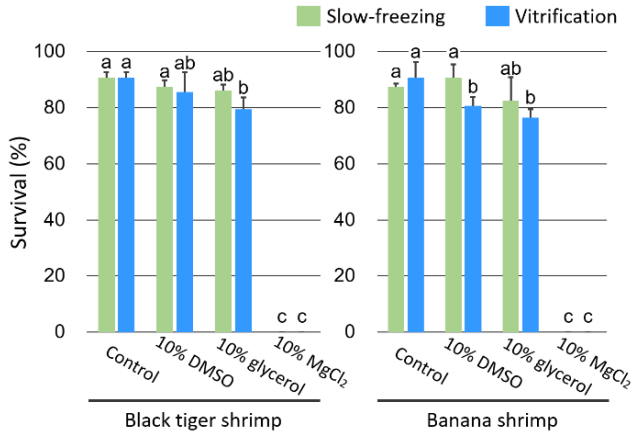

Fig. 1. Survival rates of the germ cells
Different letters indicate significant differences ($p < 0.05$).
Slow-freezing method is freezing at a rate of –1 ºC/min. The vitrification method is a rapid freezing method using liquid nitrogen after dehydration and complete replacement of intracellular water with a cryoprotectant.

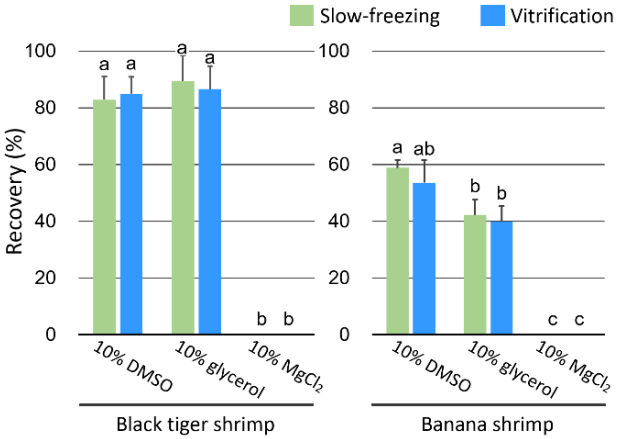

Fig. 2. Recovery rates of the germ cells
Recovery rate (%) = the number of live germ cells obtained after freezing and thawing x 100 / the number of live germ cells before freezing and thawing. Different letters indicate significant differences ($p < 0.05$).

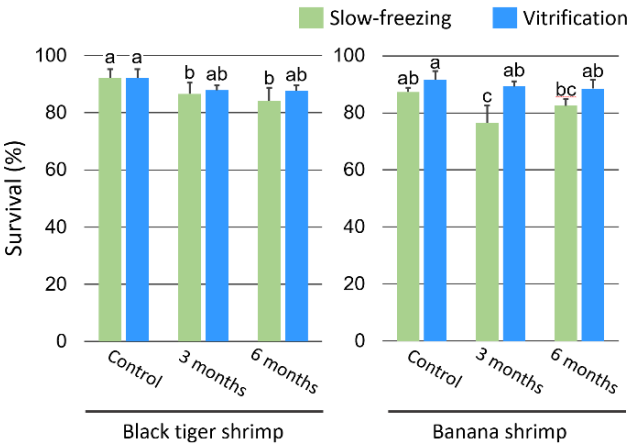

Fig. 3. Survival rates of the germ cells after long-term cryopreservation
Different letters indicate significant differences ($p < 0.05$).

Reference: Rakbanjong N et al. (2021) *Marine Biotechnology* 23: 590–601, https://doi.org/10.1007/s10126-021-10048-1

Increase of rice yield in response to phosphorus fertilizer application can be predicted by soil phosphorus retention capacity

Phosphorus (P) fertilizer application is essential for increasing crop productivity in tropical agroecosystems in sub-Saharan Africa (SSA), where P-deficient weathered soils are dominant. Farmers in SSA generally have limited capacity to purchase expensive chemical fertilizers. Therefore, P fertilizer should be efficiently applied to croplands with high response to P fertilizer application based on soil diagnosis. Soils have the capacity to fix soluble P (P retention capacity). It causes the immobilization of applied P soon after fertilizer application and decreases P availability for crops. However, there is little quantitative information on the relationship between soil P retention capacity and crop response to P fertilizer application in P-deficient soils in SSA. In this study, we clarified the relationship between soil P retention capacity and rice yield when P fertilizer was applied in the central highlands of Madagascar. Furthermore, soil physicochemical properties were investigated to verify whether our finding can be applied to other regions in SSA.

Multi-site field trials were conducted to evaluate the response of rice yield to the application of P fertilizer (ΔYield) at farmers' P-deficient paddy fields in two communes (A and B) in the central highlands of Madagascar. The ΔYield ranged from −0.4 to 2.1 t ha^{-1} among the fields and it was better predicted by soil P retention capacity than by soil available P content of the fields (Fig. 1). The ΔYield decreased with increasing soil P retention capacity. There was no response of rice yield to P fertilizer application when soil P retention capacity was higher than 35% in Commune A with mean temperature of 22.2°C during the cultivation period. On the other hand, the increase in rice yield by P fertilizer application was not observed when soil P retention capacity exceeded 53% in Commune B with mean temperature of 20.8°C. Multiple regression analysis revealed that active aluminum (oxalate-extractable Al, Alox) content was the most important factor of soil P retention across all the soils collected from 213 paddy fields in the central highlands of Madagascar (Table 1). This indicates that rice plants grown on soils with higher Alox and P retention capacity are less sensitive to P fertilizer application.

We found that the increase in rice yield in response to P fertilizer application can be predicted by soil P retention capacity. Our finding can help farmers facing P deficiency to identify the most responsive fields to P fertilizer prior to its application and, thus, to utilize efficiently a limited amount of P fertilizer in their fields. Since soils with Alox and low available P content are often seen in SSA, our finding is applicable to wide regions in SSA other than Madagascar. Further study should verify its applicability on different crops.

(T. Nishigaki, Y. Tsujimoto, H. Asai,
T. Rakotoson [University of Antananarivo (UA)], M. Rabenarivo [UA],
A. Andriamananjara [UA], H.B. Andrianary [UA],
H. Rakotonindrina [UA], T. Razafimbelo [UA])

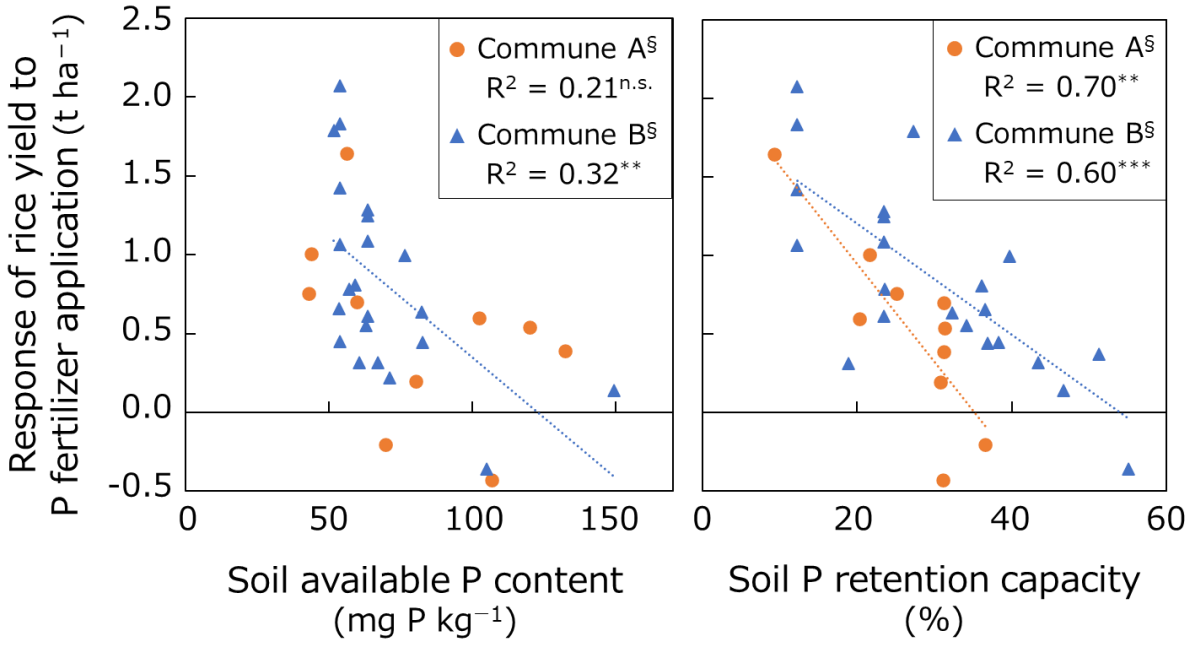

Fig. 1. Relationship between response of rice yield to P fertilizer application and soil available P content and soil P retention capacity

Yield increase in response to P fertilizer application was calculated by the difference between the rice yields of N fertilizer plot and N+P fertilizer plot in the field trials. N fertilizer was applied at 80 kg N ha^{-1} as urea, while P fertilizer was applied at 50 kg P ha^{-1} as triple super phosphate. Soil available P content was determined by acid ammonium oxalate extraction method. §Mean temperature during the cropping period was 22.2℃ and 20.8℃ at Communes A and B, respectively. ***$p < 0.001$, **$p < 0.01$, n.s. $p > 0.1$.

Table 1. Standard partial regression coefficients for soil P retention capacity and soil physicochemical properties

Alox¶	Clay	Feox¶	Base saturation
0.646***	0.305***	0.184***	0.173***

Multiple regression analysis detected soil physicochemical properties which significantly controlled soil P retention capacity for soils collected from 213 paddy rice fields in the central highlands of Madagascar. ¶Oxalate-extractable Al and Fe content. ***$p < 0.001$.

Reference: Nishigaki T et al. (2021) *Geoderma* 402: 115326, https://doi.org/10.1016/j.geoderma.2021.115326

A model for estimating soil phosphorus availability in diverse tropical ecosystems by deep learning

Since soil phosphorus (P) availability is low in tropical regions, it is necessary to accurately assess the soil P availability and implement appropriate nutrient management to realize sustainable crop production and land use. So far, we have developed a method to rapidly assess oxalate-extractable P (Pox) using visible and near-infrared (Vis-NIR) spectroscopy (JIRCAS Research Highlights 2019: "Soil phosphorus availability for rice plants can be rapidly estimated by laboratory visible and near-infrared spectroscopy"). However, this method based on partial least squares (PLS) regression strongly depends on the spectral characteristics of the training dataset, and thus, building a single model is difficult in soils with different land uses (paddy fields, crop fields, forests, etc.) and meteorological conditions. On the other hand, deep learning, in which the machine automatically discriminates wavelength characteristics, can develop a comprehensive model independent from land use. Deep learning requires a large amount of training data, but higher predictive accuracy than PLS regression can be expected. In this study, we aimed to develop a single model for estimating soil Pox in various tropical ecosystems by deep learning of spectral data.

Soil samples (n = 318) were collected from the surface layer (0–15 cm depth) in rice fields, crop fields, forests, fallow lands, and bare lands in the east coast and the central highlands of Madagascar (110–1,667 m above sea level). The spectral data was measured in the Vis-NIR region (400–2400 nm) in a dark room using a portable spectroradiometer (FieldSpec, ASD Inc.) for 2 mm sieve-passing air-dried soil. The content of soil available P was determined by acid ammonium oxalate method (Pox). The deep learning model trained the relationship between spectral data and soil Pox content using a one-dimensional convolutional neural network (1D-CNN). The 1D-CNN model can be applied to soil Pox estimation for diverse ecosystems, and its accuracy (R^2 = 0.878) is higher than that of PLS model (R^2 = 0.792) (Fig. 1). Based on the sensitivity analysis, the 1D-CNN model has high sensitivity of related wavebands (432, 590, 1433 nm) of iron oxide and water content in the soils, which are in line with PLS regression coefficients. This result suggests that these wavebands are strongly associated with the soil Pox estimation across diverse ecosystems (Fig. 2).

The developed 1D-CNN model using soil spectral data enables safe and quick estimation of soil Pox without chemical analysis, and can be used for designing optimum fertilizer application. Since the dataset for the current model covers a range of soil types and elevations in the tropics, the model can be also applied to tropical regions other than Madagascar.

(K. Kawamura, T. Nishigaki, Y. Tsujimoto,
A. Andriamananjara [University of Antananarivo (UA)], H. Rakotonindrina [UA],
M. Rabenarivo [UA], T. Razafimbelo [UA])

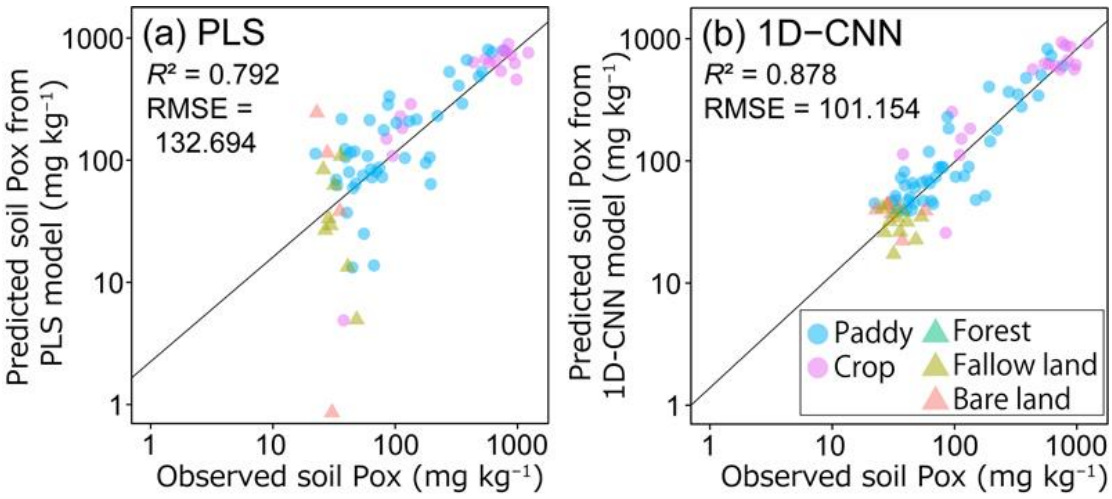

Fig. 1. Relationship between observed and predicted values of soil oxalate-extractable phosphorus (Pox) using (a) PLS model and (b) 1D-CNN model

The *x*- and *y*-axes are displayed on a log scale. RMSE: Root mean squared error.

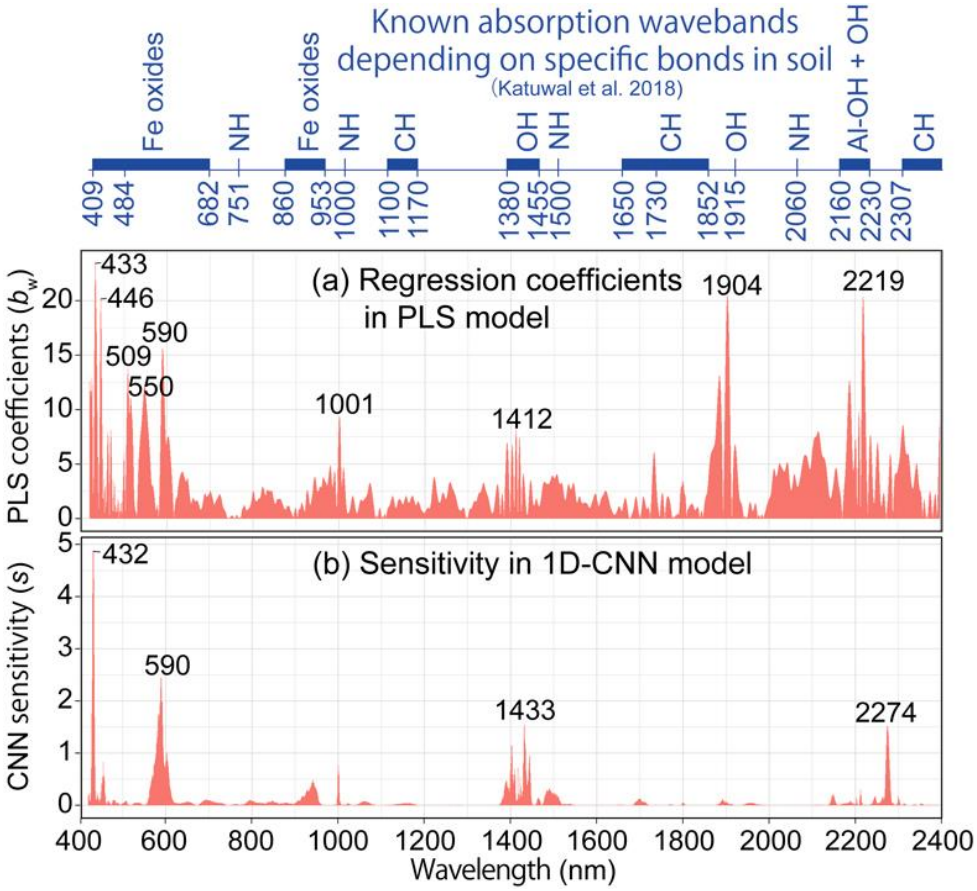

Fig. 2. (a) Regression coefficients in PLS model and (b) sensitivity in 1D-CNN model

Red lines and numbers: Importance and wavelength in the estimation of soil availability (Pox). Fe oxides are the absorption wavelengths of iron oxide. OH is the absorption wavelength of the water content.

Reference: Kawamura et al. (2021) *Remote Sensing* 13: 1519, https://doi.org/10.3390/rs13081519

Efficient phosphorus application strategy to improve rice yields under cold stress-prone and P-deficient environments

Despite a general perception that phosphorus (P) deficiency delays phenological development in annual crops, the impacts of interaction between this phenological delay and climatic conditions on crop productivity remain poorly understood. On-farm experiments were conducted in the central highlands of Madagascar, where P deficiency and late-season low temperature stress frequently restrict rice yields. Rice X265 was grown under four different fertilizer treatments with different combinations of N and P during early and late transplanting dates (ETP and LTP, respectively). Plants subjected to no fertilizer or single N treatments (-P) showed delayed heading by 9–16 days relative to the single P and N and P combined plots on average (Table 1). The delay in phenological development without P application (-P) and the delay in transplanting date (LTP) additively increased the risk of low temperature stresses at the heading periods (Fig. 1). As a result, -P plots at LTP increased the cooling degree days and spikelet sterility while the delay in phenological development without P application little affected the cooling degree days and spikelet sterility when transplanted early or ETP (Fig. 2). With this significant interaction between P application and transplanting dates on cold stresses, the effect of P on rice yield was much greater in LTP than in ETP because P application alleviated not only P deficiency but low temperature stress as well by shortening day to heading (Table 1). This study provides field evidence that the effects of P application on rice yield were greatly dependent on transplanting date via their impact on phenological development under P-deficiency in climate stress-prone environments. Changes in phenological development due to plant nutrient status and its interaction with climate-induced stress needs further attention for improving fertilizer management practice.

(Y. Tsujimoto, A.Z. Oo, T. Nishigaki,
B. Andrianary [University of Antananarivo (UA), LRI],
H. Rakotonindrina [UA, LRI], M. Rabenarivo [UA, LRI], N. Ramifehiarivo [UA, LRI],
H. Razakamanarivo [UA, LRI], T. Rakotoson [UA, LRI])

Table 1. Effect of P application and transplanting date on days to heading and yield of rice grown on P-deficient fields

		Days from transplanting to heading			Yield (t ha^{-1})		
		-P	+P	Difference between +P and -P	-P	+P	Difference between +P and -P
ETP	Field1	111	95	<u>-16</u>	2.2	3.1	<u>0.8</u>
	Field2	110	98	<u>-11</u>	2.4	3.2	<u>0.8</u>
LTP	Field1	109	96	<u>-12</u>	1.9	3.1	<u>1.2</u>
	Field2	105	96	<u>-9</u>	1.8	3.1	<u>1.3</u>

-P indicates the means of the plots without fertilizer and with N applied as urea at the rate of 80 kg N ha^{-1}. +P indicates the means of plots with P applied as triple super phosphate at the rate of 50 kg P_2O_5 ha^{-1} and with N and P combined.

ETP refers to early transplanting plots (November 28-29). LTP refers to late transplanting plots (December 27-30).

Underlined values indicate significant differences between -P and +P plots at 5% by Tukey HSD.

ANOVA detected a significant interaction between P treatment and transplanting dates on yield.

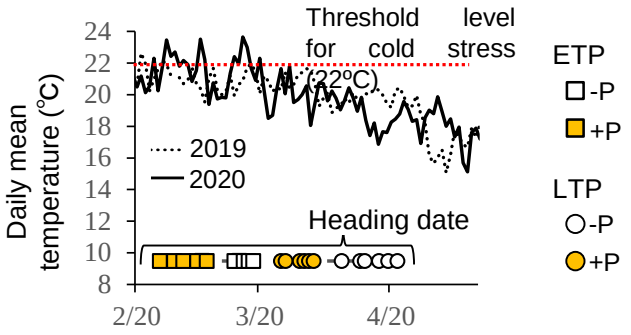

Fig. 1. Changes in daily mean temperatures at the heading periods as affected by transplanting dates and P application

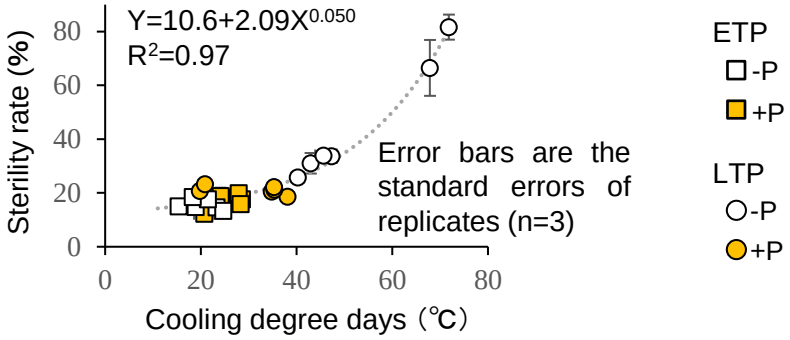

Fig. 2. Effect of transplanting dates and P application on the cooling degree days (CDD) and spikelet sterility

CDD is the sum of daily mean temperatures below 22ºC from 15 days before to 7 days after heading.

Reference: Andrianary et al. (2021) *Field Crops Research* 271: 108256, https://doi.org/10.1016/j.fcr.2021.108256, and Rakotoson et al. (2022) *Field Crops Research* 275: 108370, https://doi.org/10.1016/j.fcr.2021.108370

Meta-analysis reveals the effect of fertilizer application on upland rice cultivation in Africa

Rainfed upland is one of the dominant ecosystems for rice production in sub-Saharan Africa, where yields are very low (approx. 2.1 t ha^{-1}). To overcome such low productivity, fertilizer application is necessary, and its effective use is key for improving rice yield and farmer's livelihood. Previous studies often reported that fertilizer application did not result in sufficient yield increase. It is partly because yield gain with fertilizer could be affected by biophysical factors such as precipitation and soil texture; however, their interaction remained poorly understood. Hence, a meta-analysis was performed for the dataset collected from fertilizer trials conducted in 8 countries in sub-Saharan Africa, where the environmental backgrounds varied considerably, in order to quantify the effect of soil texture and precipitation on yield gain with fertilizer.

The dataset was composed of 151 paired observations of control and fertilizer treatment from fertilizer trials using NERICA 4 from 8 countries (Table 1). Soils were classified into low clay soil (≤ 20% clay content) and high clay soil (> 20% clay content). Yield gain with fertilizer application (YG), i.e., the yield difference between fertilizer treatment and control, was evaluated in relation to nitrogen (N), phosphorus (P) and potassium (K) fertilizer application rates and the amount of precipitation. Regression analysis showed no correlation between YG and P and K fertilization rates ($p > 0.05$, data not shown). Precipitation closely correlated with YG, irrespective of soil type ($p < 0.001$, Fig. 1 left). N fertilizer rate was correlated with YG in high clay soil, ($p < 0.001$, Fig. 1 right,) but not in low clay soil ($p > 0.05$). Bayesian estimation clarified that YG would increase by 0.168 and 0.145 t ha^{-1} for low and high clay soil with a 100 mm increase in precipitation (Table 2). YG was also expected to increase by 0.653 t ha^{-1} in high clay soil with a 100 kg increase in N fertilizer rate, but in low clay soil, 95% posterior credibility intervals included zero, indicating that YG did not always increase with N fertilizer rate. Overall, these results recommend the fine-tuning of N fertilizer input based on soil type and expected precipitation.

The obtained results will allow the policy maker or private sector to predict the fertilizer-suitable areas for technical dissemination and commercial sale at the regional and/or national level. However, trends at the regional level may not be directly applicable to individual fields or to regions where the yields are constrained by other nutrient deficiencies such as phosphorus deficiency etc. In addition, further assessments are required for varieties other than NERICA 4.

(H. Asai, K. Kawamura, K. Saito [Africa Rice Center])

Table 1. Description of fertilizer trials using upland rice (NERICA 4) in 8 countries in Africa

Country	Num.	Soil type (clay content)[2)]		Fertilizer effect			
		Low clay (≤20%)	High clay (>20%)	NPK	N	P	K
Gambia	4	4	0	4	0	0	0
Guinea	2	2	0	2	0	0	0
Mali	2	2	0	2	0	0	0
Benin	65	65	0	53	12	0	0
Uganda	50	0	50	20	10	10	10
Nigeria	15	3	12	0	13	1	1
Kenya	12	12	0	2	6	4	0
Madagascar	1	0	1	1	0	0	0
Total	151	88	63	84	41	15	11

[1)] Database：https://ars.els-cdn.com/content/image/1-s2.0-S0378429021002306-mmc1.xlsx

[2)] Tanaka et al. (2017)

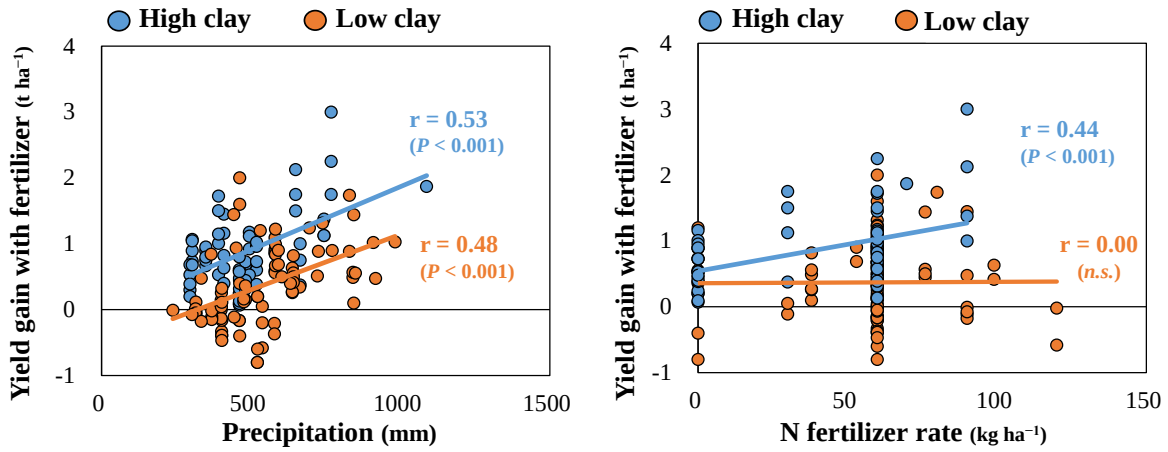

Fig. 1. The relationship of yield gain with fertilizer (YG) with precipitation (left) and N fertilizer application rate (right)

Table 2. Posterior probability distribution of the effect of precipitation and N fertilizer rate on yield gain with fertilizer under different soil types

Soil type	Precipitation (t ha^{-1} 100mm^{-1})			N fertilizer rate (t ha^{-1} 100kg^{-1})		
	Average	95% credible interval [1)]		Average	95% credible interval [1)]	
		2.5%	97.5%		2.5%	97.5%
High clay	0.145	0.068	0.22	0.653	0.253	1.05
Low clay	0.168	0.103	0.236	0.164	−0.352	0.679

[1)] Credible interval is the range containing a 95% percentage of probable values estimated by Bayesian statistics.

Reference: Asai et al. (2021) *Field Crops Research* 272: 108284. https://doi.org/10.1016/j.fcr.2021.108284

Introducing vegetables upstream of irrigation areas may increase farm income and lead to equitable water distribution

In sub-Saharan Africa, the development of irrigated rice techniques have been promoted in response to increasing demand for rice, resulting in high yields. However, in recent years, the decline in the amount of irrigation water due to unstable river flows and deteriorating irrigation facilities, as well as uneven irrigation water distribution between upstream and downstream, have emerged as factors constraining further rice production and farmer economy. On the other hand, demand for horticultural crops is growing in local markets, creating a condition for farmers to increase their incomes through agricultural diversification.

We examined the effects of changing the cropping system on water-saving, productivity, and profitability, based on the idea that converting double rice cropping to rice-upland crop system will lead to more efficient water use without sacrificing farm income. The field experiments and farmer surveys were conducted in the Lower Moshi Irrigation Scheme in northern Tanzania.

The main results are summarized as follows. First, conversion of rice to maize reduces irrigation water by 77%. Vegetables, which require the least number of irrigation days, are expected to save even more water (Table 1). Second, land productivity measured by value added (gross output minus non-labor expenditures) is higher in the order of vegetables > lowland rice > lowland maize > upland maize, and labor productivity is higher in the order of lowland maize > upland maize > vegetables > lowland rice. In case of strict land constraints, vegetables and rice are economically rational, while for farmers facing labor shortage, maize is advantageous over rice and vegetables (Fig. 1). Third, income not counting family labor as a cost is higher in the order of vegetables > lowland rice > lowland maize > upland maize. When taking family labor into account as a cost, profit is higher in the order of lowland rice > vegetables > lowland maize > upland maize. If vegetables are introduced after rice in lowland, the income can be expected to exceed that of double rice system. However, for households with high opportunity cost for family labor, the economic incentive to introduce vegetables is weak (Table 2).

The above findings suggest that in irrigation schemes where rice cultivation has been increasingly constrained due to water shortage, introducing vegetables upstream and allocating surplus irrigation water downstream for rice may lead to efficient use of irrigation and farmer income increase for the irrigation scheme as a whole. It should be noted that first, to introduce commercial vegetables, due consideration of water drainage techniques, marketing arrangements, and risk management is crucial; and second, reducing staple food crops (rice and maize) and specializing in commercial vegetables, which have large profit fluctuations and no storage potential, may reduce food security at the household level.

(*S. Yokoyama*)

Table 1. Estimation of irrigation water requirements by crop (per crop season, 2018-19)

	Lowland rice[1]	Lowland maize[1]	Vegetables[2]
Irrigation period (day)	110	25	13.2
Daily irrigation amount (mm/day)	13	13	NA
Total irrigation amount (mm)	1,430	325	NA

1) Canal irrigation. Measured in cultivation trial. 2) Interviews (n=9) in the irrigation scheme, vegetables are grown by private pump irrigation due to lack of canal water supply. The pumps used by the farmers have a capacity of less than 15 mm/day. African nightshade, amaranth, onion, bell pepper, Chinese cabbage, and squash are produced for market.

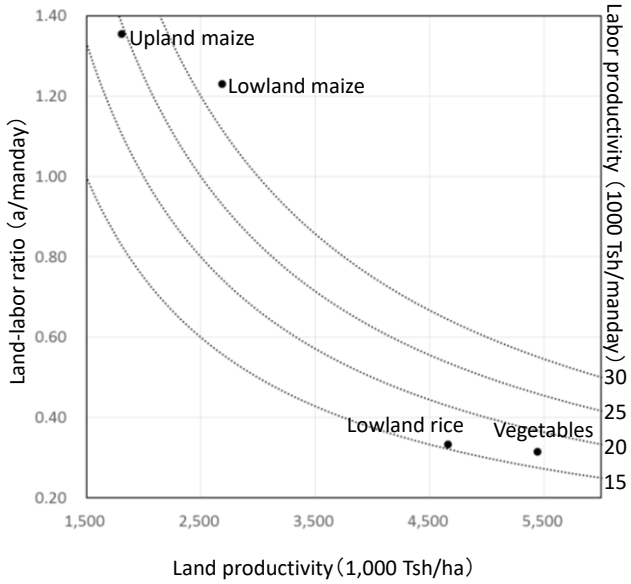

Fig. 1. Land and labor productivity by crop

1) Horizontal axis is land productivity (value added/area)
2) Vertical axis is land labor ratio (area/labor input)
Higher values indicate land-use crops, lower values indicate labor-intensive crops
3) The dotted line is the iso-labor productivity curve
Labor productivity (value added/labor input) = land productivity x land-labor ratio
4) Tsh is Tanzanian shilling
1 Tsh = 0.047 yen (November 18, 2019)

Table 2. Production cost and management indicators by crop (2018-19)

	Rice	Maize		Vegetables
Condition of irrigation （Sample number）	Irrigated lowland (78)	Irrigated lowland after rice (10)	Irrigated upland (5)	Well irrigation (9) [1]
Farm size (ha)	0.83	0.94	2.3	1.2
Surveyed plot (ha)	0.29	0.54	1.04	0.23
Yield (t/ha)	6.62	5.71	3.74	NA
Gross product: A (1000 Tsh/ha)	5,919	3,847	2,411	6,243
Cost (1000 Tsh/ha)				
Current input,	1,263	1,165	605	802 [2]
Hired labor	973	395	403	1,165
Family labor: B [3]	480	541	378	2,088
Total: C	2,717	2,101	1,386	4,056
Income：A – C + B (1,000 Tsh/ha)	3,682	2,287	1,405	4,276
Profit：A – C (1,000 Tsh/ha) [4]	3,202 (0.44)	1,746 (0.95)	1,027 (1.19)	2,188 (2.28)

1) Private pump irrigation using shallow well. 2) Irrigation cost is imputed based on the rate for lowland maize. 3) Imputed based on market wage rate. 4) The number in parentheses is the coefficient of variation, representing the variability of profit as a proxy indicator of risk.

Reference: Yokoyama (2022) *Japanese Journal of Farm Management* 59(4): 69–74.
Figure and tables reprinted/modified with permission.

Information on the genetic diversity in agronomic traits of Thai *Erianthus* germplasm under multiple ratooning systems

Erianthus spp., one of the genetic resources of a closely related genus of sugarcane, show considerable potential as breeding material for sugarcane improvement and as a new biomass crop due to its high biomass productivity under multiple ratooning systems. Strong ratooning ability is a desirable trait not only because it is key to improving sugar and fiber production, but also because it avoids the need for frequent replanting, thus playing an important role in ensuring sustainable cultivation with lower production costs and energy input as well as in preventing soil erosion. However, the lack of scientific information on the genetic diversity of agronomic traits, especially under multiple ratooning systems, prevents us from the effective breeding use of this genetic resource. To utilize *Erianthus* for sugarcane breeding and biomass production effectively, JIRCAS and Khon Kaen Field Crops Research Center, Department of Agriculture, Thailand, collected *E. arundinaceus* and *E. procerus* germplasm from all over Thailand, which is presumed to host diverse *Erianthus* genetic resources due to its location between India, Indonesia, and China. In this study, we evaluated the genetic variation of important agronomic traits in Thai *Erianthus* germplasm in multiple ratooning systems as an initial screening of a large number of clones with diverse genetic backgrounds to obtain basic information and identify potentially valuable materials for breeding of sugarcane and new biomass crop in Thailand.

The 98 *E. arundinaceus* and 32 *E. procerus* clones collected in Thailand showed large genetic variation in agronomic traits related to biomass productivity under multiple ratooning systems, and many clones have higher dry matter yield than sugarcane variety and Napier grass (Fig. 1). There is also a large variation in Multiple-Ratoon Index (the ratio of 3rd ratoon to 1st ratoon), and many clones provided better dry matter yields and lower yield reductions in ratoon crops than a sugarcane cultivar, highlighting the importance of identifying and using clones as breeding materials with excellent dry matter yields and Multiple-Ratoon Index. Furthermore, the dry matter yield showed a strong genetic correlation with stalk number, but not with single stalk weight, stalk diameter, or Brix, allowing selection of breeding materials with higher dry matter yield in multiple ratooning systems and superior single stalk weight, stalk diameter, or Brix. Based on the results, clones with various combinations of advantageous traits were identified as promising genetic resources.

The information about agronomic traits in the multiple ratooning systems provided in this study, as well as the clones selected, should enhance the use of *Erianthus* germplasm in sugarcane breeding in Thailand and around the world. Furthermore, our results could also be used to explore the practical utilization of *Erianthus* itself as a biomass crop.

(Y. Terajima, A. Sugimoto, H. Takagi, W. Ponragdee [Khon Kaen Field Crops Research Center (KKFCRC)], T. Sansayawichai [KKFCRC], A. Tippayawat [KKFCRC], S. Chanachai [KKFCRC], M. Ebina [National Agriculture and Food Research Organization], H. Hayashi [University of Tsukuba])

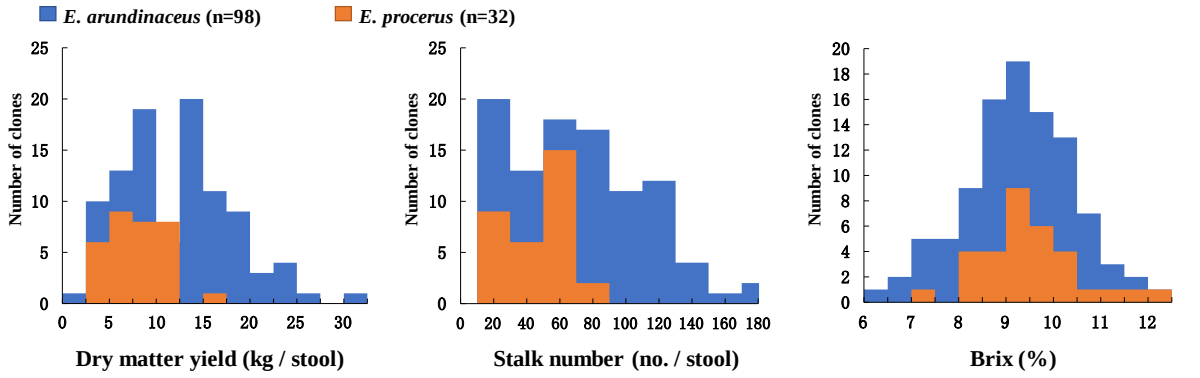

	Avg.	Multiple-Ratoon Index
E. arundinaceus	12.1	0.63 (0.10 - 1.81)
E. procerus	8.0	0.33 (0.13 - 0.79)
Sugarcane	5.2	0.11
Napier	6.6	0.16

	Avg.	Multiple-Ratoon Index
E. arundinaceus	80.3	1.06 (0.33 - 2.19)
E. procerus	57.6	0.66 (0.31 - 1.28)
Sugarcane	18.3	0.94
Napier	38.1	0.43

	Avg.	Multiple-Ratoon Index
E. arundinaceus	9.3	1.13 (0.57 - 1.96)
E. procerus	9.5	1.14 (0.71 - 1.59)
Sugarcane	19.1	0.78
Napier	9.1	1.07

Fig. 1. Agronomic traits in *E. arundinaceus* and *E. procerus* under multiple ratooning systems

The experiment was conducted in KKFCRC. Each experimental plot was planted with a single stool with 2 m inter-hill and row spacing and three replications. The field was planted in June 2011 and harvested from the end of February to early March in 2012 to 2015. The data in the figure used the average values of the four years of harvesting. The Multiple-Ratoon Index defined the ratio of third ratoon crop to first ratoon crop values. Sugarcane variety TPJ03-452 is a BC_1 hybrid derived from interspecific hybridization between sugarcane and *S. spontaneum* and registered in 2015 as a cultivar for sugar and fiber production in northeast Thailand. King Napier is a Napier grass variety used commercially in northeast Thailand.

Table 1. Genetic correlation coefficient between dry matter yield and other agronomic traits

Traits	*E. arundinaceus* (*n=98*)	*E. procerus* (*n=32*)
Stalk number	0.958 **	0.541 **
Single stalk weight	-0.240 *	0.295 n.s.
Stalk length	0.932 **	0.210 n.s.
Stalk diameter	0.032 n.s.	0.149 n.s.
Brix	-0.502 **	0.019 n.s.

The genetic correlation coefficients were calculated using four-year average values for each trait. ** and * indicate significant differences at $p = 0.01$ and $p = 0.05$, respectively; n.s. not significant

Fig. 2. Breeding materials with high dry matter yield under multiple ratooning systems

The pictures were taken in March 2013 at the Khon Kaen Field Crops Research Center. The pictures show, from left to right, *E. arundinaceus* ThE03-7, ThE10-6, and *E. procerus* ThE99-133.

Reference: Terajima et al. (2022) *Crop Science*, 62: 1531–1549. https://doi.org/10.1002/csc2.20697

Development of a simple shoot-tip grafting method for virus-free passion fruit

Passion fruit (*Passiflora edulis*) is the third most important tropical fruit produced in Japan after pineapple and mango. The plant consists of a woody vine that grows rapidly under warm humid conditions, while fruits can be harvested about five months after planting. Commercial cultivation of passion fruit is therefore possible before winter, even in temperate regions where survival is not possible during the cold months. As a result, cultivation of passion fruit is gaining increasing attention in Japan as one of several alternative crops to replace those increasingly suffering from heat stress under climate change.

Management of virus diseases is one of the most important subjects in commercial production of passion fruit. The basic treatment for virus disease control is to introduce virus-free seedlings. However, depending on the type of virus, it is often difficult to detect the external symptoms of the disease such as those caused by the Passiflora latent virus (PLV), thus making the procurement of virus-free plants challenging. In such cases, infected plants must be made virus-free and used as mother trees for propagation. To address the above problem, a technology for virus-free propagation of passion fruit using a simple shoot-tip grafting method has been developed (Fig. 1).

The shoot-tip was *in vivo* grafted and examined to obtain PLV-free passion fruit from infected plants. The scion length required to eliminate PLV was ≤ 2 mm (Table 1). The method required no aseptic handling and the procedure was relatively simple, and resulted in more than ten grafts in one hour, allowing it to be conducted at an individual farm level. Rapid growth of the scion after grafting was also observed due to the use of fully established seedlings as rootstock. Leaf samples for analysis of PLV infection could therefore be obtained about two months after grafting with fruit harvest possible about four months later (Fig. 1).

In vivo shoot-tip grafting was conducted with a scion length of 0.5–1 mm from September to November to determine the optimal air temperature conditions. The graft success rate increased from 18% to 58% with a decrease in the average air temperature from September (28.6°C) to November (23.3°C), although there was no significant difference in PLV-free rates between months (73% to 80%) (Table 2). Accordingly, *in vivo* shoot-tip grafting of passion fruit is not recommended under high air temperature conditions.

The effect of scion shoot storage conditions was also examined, revealing that *in vivo* shoot-tip grafting using shoots stored for one day could be performed without difficulty, whereas the rate of graft success and PLV-free rate were close to those obtained using shoots selected less than 30 min before (Table 3). These findings suggest that with this method, virus-free plants can be obtained using PLV-infected shoots selected in the field one day earlier. In conclusion, our *in vivo* shoot-tip grafting technique is useful for eliminating PLV from infected plants without any aseptic treatment or specific equipment, and could therefore contribute as a practical method to control virus diseases in passion fruit.

(T. Ogata, S. Yamanaka)

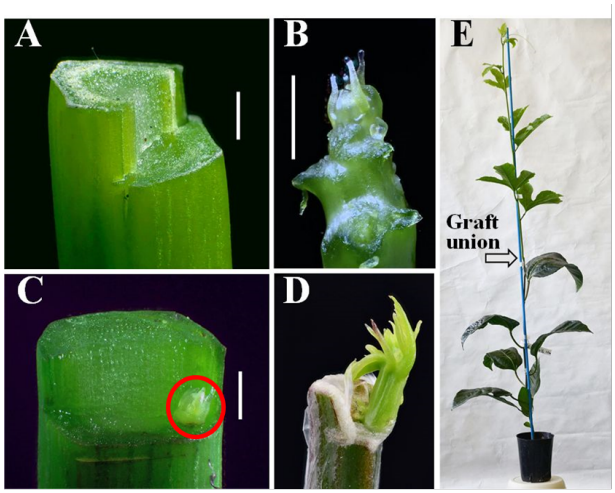

A: A 1~2-mm-long half-cylinder section of the cut end of a rootstock was removed using a razor blade.
B: The shoot-tip was used as a scion, with young leaves and leaf primordia removed before excision.
C: The cambium on the L-shaped cut end of the rootstock to which the excised shoot-tip (scion) was attached. The graft was then covered with laboratory film to prevent drying.
D: Sprouting of the scion about one month after *in vivo* shoot-tip grafting. The sprouting scion self-pierced the laboratory film, so removal of the the film was not necessary.
E: The growing scion about two months after micrografting, ready for virus detection.

Fig. 1. *In vivo* shoot-tip grafting of passion fruit
Bars in A, B, and C: 1 mm.

Table 1. Effect of shoot-tip (scion) length on the elimination of Passiflora latent virus (PLV) via *in vivo* shoot-tip grafting

Shoot-tip (scion) length (mm)	Shoot-tip grafting		PLV
	Number of grafts	Success rate (%)	Virus-free rate (%)
1	8	63	60
2–3	5	100	40
5	8	100	0
Significance[a]		*	*

[a]: 5% level in Fischer's exact test.

Table 2. Effect of grafting time on grafting success and elimination of Passiflora latent virus (PLV) via in vivo shoot-tip grafting

Grafting time	Shoot-tip grafting			PLV	Air temperature (ºC)		
	Number of grafts	Success rate(%)	Days to sprouting	Virus-free rate(%)	Max.	Ave.	Min.
September	60	18	32±11	73	35.9	28.6	24.9
October	24	33	31±22	80	30.4	24.4	21.1
November	65	58	29±19	73	29.0	23.3	20.1
Significance[a]		*		NS			

[a]: 5% level in Fischer's exact test.

Table 3. Effect of scion shoot storage conditions on the elimination of Passiflora latent virus (PLV) via in vivo shoot-tip grafting

Storage conditions	Shoot-tip grafting		PLV
	Number of grafts	Success rate (%)	Virus-free rate (%)
5ºC 1day	17	59	80
25ºC 1day	18	50	56
Significance[a]		NS	NS

[a]: 5% level in Fischer's exact test.

Reference: Ogata T and Yamanaka S (2021) *Horticulture Journal*, https://doi.org/10.2503/hortj.UTD-259

Japan International Research Center for Agricultural Sciences

Headquarters (Tsukuba)
1-1 Ohwashi, Tsukuba, Ibaraki
305-8686, JAPAN
TEL : +81-29-838-6313
FAX : +81-29-838-6316

Tropical Agriculture Research Front (TARF)
1091-1 Maezato-Kawarabaru, Ishigaki
Okinawa, 907-0002, JAPAN
TEL : +81-980-82-2306
FAX : +81-980-82-0614

https://www.jircas.go.jp/